# An Animated Tectonic Reconstruction of Southwestern North America since 36 Ma

**Nadine McQuarrie**
**Brian P. Wernicke**
*Division of Geological and Planetary Sciences, MS 100-23, California Institute of Technology, Pasadena, CA 91125*

## ABSTRACT

We present tectonic reconstructions and an accompanying animation of deformation across the North America/ Pacific plate boundary since 36 Ma. Intraplate deformation of southwestern North America was obtained through synthesis of kinematic data (amount, timing and direction of displacement) along three main transects through the northern (40° N) central (36°-37° N) and southern (34° N) portions of the Basin and Range province. We combined these transects with first-order plate boundary constraints from the San Andreas fault and other areas west of the Basin and Range. Extension and strike-slip deformation in all areas were sequentially restored over 2 m.y. (0 to 18 Ma) to 6 m.y. (18 to 36 Ma) time intervals using the ArcGIS program. Regions where the kinematics are known constrain adjacent areas where the kinematics are not well defined. The process of sequential restoration highlighted misalignments, overlaps or large gaps in each incremental step, particularly in the areas between data transects, which remain problematic. Hence the value of the reconstructions lies primarily in highlighting questions that might not otherwise be recognized, and thus they should not be viewed as a 'final product.'

The new sequential reconstructions show that compatible slip along the entire N-S extent of the inland right –lateral shear zone from the Gulf of California to the northern Walker Lane is supported by available data, and that the east limit of shear has migrated westward with time. The reconstructions also highlight new problems regarding strain compatible extension east and west of the Sierra Nevada/Great Valley block and strain compatible deformation between southern Arizona and the Mexican Basin and Range. Results show ~235 of extension oriented ~N78°W in both the northern (50% extension) and central (200% extension) parts of the Basin and Range. Following the initiation of EW to SW-NE extension at 15-25 Ma (depending on longitude), a significant portion of right-lateral shear associated with the growing Pacific-North America transform jumped into the continent at 10-12 Ma, totaling ~100 km oriented N 25 W, for an average of about 1 cm/yr since that time.

## INTRODUCTION

The large-scale horizontal velocity field at the earth's surface is one of the main predictions of physical models of lithospheric deformation (e.g. England and McKenzie, 1982). Two-dimensional, cross-sectional models of finite deformation of

---

Now at: Department of Geosciences, Guyot Hall, Princeton University, Princeton, NJ 08544 mountain belts incorporating strong heterogeneity in rheologic parameters have been developed over the last decade (e.g. Lavier and Buck, 2002; Braun and Pauselli, 2004). Owing to advances in computation, fully three-dimensional models of plate boundary deformation zones, incorporating both horizontal and vertical variations in lithospheric rheology, will soon become common. Thus a key observational frontier will be the determination of precise displacement vector fields of continental deformation in order to test these models. The most dramatic recent improvement in obtaining such velocity fields has been the advent of spaced-based tectonic geodesy (especially using continuous GPS), which is yielding velocity fields that are unprecedented in terms of both the scale of observation and the accuracy of the velocities. These data have already been used as tests for physical models in southwestern North America (e.g. Bennett et al., 1999; 2003; Flesch et al., 2000) and elsewhere (e.g. Holt et al., 2000). Substantial progress has also occurred over the last decade in determining longer-term velocity fields using the methods of plate tectonics and regional structural geology. These longer-term displacement histories are essential for addressing the question of how the lithosphere responds to major variations in plate geometry and kinematics (e.g. Houseman and England, 1986; England and Houseman, 1986), because such variations occur on the million-year time scale.

Plate tectonics is a precise method for constraining the overall horizontal kinematics of plate boundaries, using seafloor topographic and magnetic data in concert with the geomagnetic timescale. For the diffuse deformation that characterizes the continental lithosphere along plate boundaries, however, tectonic reconstruction at scales in the 100 km to 1000 km range is not as straightforward. It is based primarily on structural geology and paleomagnetic studies, and requires the identification of large-scale strain markers and consideration of plate tectonic constraints (e.g. Wernicke et al., 1988; Snow and Wernicke, 2000; McQuarrie et al., 2003). Regional strain markers within the continents may not exist in any given region, and even if they do they may not be amenable to accurate reconstruction at large scale.

In southwestern North America, a zone of plate boundary deformation on the order of 1000 km wide is developed along the plate boundary. In mid-Tertiary time (36 Ma) this boundary was strongly convergent, with the Farallon plate subducting eastward beneath the North American plate. Beginning at about 30 Ma, the Pacific-Farallon ridge came in contact with the North American plate. Since then, the Pacific-North America boundary has grown through the migration of triple junctions along the coast. Now, the entire margin from southern Baja California to Cape Mendocino is a transform Pacific-North America boundary, rather than a convergent Farallon-North America boundary (Atwater, 1970). This change in the configuration of the plate boundary is both relatively simple and profound, making southwestern North America an ideal laboratory for investigating how continental lithosphere responds to changes in relative plate motion.

Refined plate tectonic reconstructions have provided an improved kinematic model of the change from convergent to transform motion, and have shown that there were significant variations in the obliquity of the transform after it developed. In particular, during the interval ~16 to ~8 Ma, Pacific-North America motion was highly oblique, and included a margin-normal extensional component of as much as 2 cm/yr, coeval with a rapid pulse of Miocene extension that formed the Basin and Range province (Atwater and Stock, 1998; Wernicke and Snow, 1998). At ~8 Ma, Pacific North-America motion changed to more purely coastwise motion, which appears to have changed the intraplate tectonic regime from profound extension to a more complex mixture of extension, shortening and transform motion, responsible for opening of the Gulf of California, thrust faulting of the western Transverse Ranges, and development of the San Andreas fault/eastern California shear zone, respectively.

Over the last several years high-quality, large-scale kinematic constraints, many of which resulted from decades of field work and attending debate, have become available, reaching the point where synthesis into a large-scale velocity field is feasible. A rudimentary kinematic model using many of the constraints along the plate boundary and in the plate interior was incorporated into a publicly available animation of the post-38 Ma evolution of the entire Pacific-Farallon-North America system (Atwater and Stock, 1998; animation available at http://emvc.geol.ucsb.edu/download/nepac.php).

In this paper, we synthesize the current state of information on the kinematics of the diffusely deforming North American plate since 36 Ma based on offsets of regional structural markers, and construct a strain-compatible kinematic model of the horizontal motions at 2 Myr (0-18 Ma) and 6 Myr (18-36 Ma) intervals, presented as a continuous animation. The model is by no means a "final product," as new kinematic information and testing will require significant modifications of the model. Rather, the model is an attempt to be quantitatively rigorous in a way that will be useful for comparison with large-scale, three-dimensional physical models, and for identification of issues regarding the structural kinematics that might not otherwise be detected. Thus in addition to the animation, we have constructed "instantaneous" velocity fields based on 2 Myr averages from 0 to 18 Ma, and 6 Myr averages from 18 to 36 Ma. These results are our best attempt at "paleogeodesy," presenting the geology-based kinematic model in a format similar to modern GPS velocity fields, which in turn may be quantitatively compared to physically based model velocity fields.

## METHODS

By combining regional structural constraints into a single model, the self-consistency of the model (i.e., its strain compatibility through time) provides powerful additional constraints on the kinematics, in at least three ways. The first and most important is the fact that high quality local kinematic information imposes severe constraints on its surroundings, where information may not be available. As a hypothetical example, consider a large region of oblique extension between two undeformed blocks (Figure 1). The strain and strain path need not be known for each geological element in the deforming region in order to constrain the large-scale kinematics. If the sum of fault displacements across just a single reconstruction path **p** is known, restoring point A to a position at point B, and it is known that the blocks have not rotated, then the single path imposes a strong constraint on the overall kinematics of all of the other paths between the blocks (Figure 1A).

The second additional constraint is on errors in reconstructions. In the example in Figure 1, let us suppose that the minimum value of all fault displacements along reconstruction path **p** restores the block to point B, but there is no constraint on the maximum value along the path itself. The side of the block containing A would overlap the block on the other side of the rift if the displacement along the path were in excess of AC (Figure 1B), violating the condition of strain compatibility. Therefore the displacement is constrained to be between AB and AC, rather than some value greater than AB.

A third and perhaps most useful additional constraint arises when local constraints contradict one another. For example, if reconstruction along path **q** (Figure 1A) required that point A restore to a position D, which is well within the other block, then the violation of strain compatibility forces re-evaluation of the geological constraints. The geological reconstruction for displacement along **q**, the paleomagnetic constraints on the blocks, and the presumed rigidity of the blocks cannot all be correct. Thus the exercise of regional reconstruction focuses attention on information that is most critical for improving the accuracy of the reconstruction. For southwestern North America, there is now enough high-quality local kinematic information that large-scale self-consistency of the model imposes useful additional constraints, in all of these ways.

In making the reconstruction, the methods used in the local study of Wernicke et al., (1988) and Snow and Wernicke (2000) in the Death Valley region of the central Basin and Range province were applied at large scale. In Snow and Wernicke (2000), each step in the reconstruction showed the paleoposition of existing mountain ranges. Although the reconstruction allowed for the ranges to change shape as extension is restored (i.e. the ranges may decrease in area), in our reconstruction, the mountain ranges are shown as digitized polygons that approximate: (1) the modern bedrock-alluvium contact (e.g., a typical range in the Basin and Range), (2) faults bounding individual crustal blocks (e.g., the Santa Ynez Mountains block in the western Transverse Ranges), or (3) the physiographic boundaries of large, intact crustal blocks (e.g. the Colorado Plateau). In some cases, especially where large extensional strains are involved, the reconstruction overlaps individual polygons to account for extension, essentially using the modern bedrock-alluvium contact as a geographical reference marker. Because the strain is extensional and in the case of metamorphic core complexes one range has literally moved off of the top of another, these overlaps do not violate strain compatibility.

The individual positions of polygons were restored in each 2 Myr time frame through an arcGIS script that reads and updates a table listing the kinematic data for each range. The data includes the age, amount, and direction of displacement as well as any vertical axis rotation. For the regions where kinematic data is not available, the kinematics could be defined by inserting data from proximal areas, or individual ranges could be moved by hand with the motion updated and recorded in the table using the arcGIS script. The arcGIS format and accompanying script allows for exact displacements to be incorporated into the model, as well as the individual adjustment of ranges to insure strain compatibility. The GIS script records the geographical position of the centroid of each range at each 2 Myr epoch. This allows for the data to be displayed in a variety of ways including palinspastic maps for each 2 or 6 Myr epoch, "instantaneous" velocity vectors at each 2 or 6 Myr epoch, "paths" that individual ranges take over the 36 Myr span of the reconstruction, or an animation that shows the integrated motion over 36 Myr. "Instantaneous" geology velocity fields are obtained from connecting the centroids of specific ranges at one time with the centroid of the same range in a later time.

## DATA

The primary tectonic elements in the reconstruction are large crustal blocks comprising flat-lying pre-36 Ma strata, or geologic elements that are otherwise little deformed, and the straining areas in between them. The large unstrained blocks include (Figure 2): the Great Plains/Rocky Mountains region (nominal North America reference frame); the Sierra Madre Occidental; the Colorado Plateau; the Sierra Nevada/Great Valley block; and Peninsular Ranges block. The strained areas around them include the Rio Grande rift and Basin and Range province, the Gulf of California, the Transverse Ranges, the Coast Ranges, and the Continental Borderlands province offshore of southern California and Baja California.

The constraints used in the reconstruction are organized into six major categories (Tables 1 to 6). The first covers a range-by-range reconstruction path across the northern Basin and Range near latitude 40°N (Figure 3 and Table 1). The second includes a similar reconstruction path across the central Basin and Range near latitude 37°N (Figure 4 and Table 2). These two reconstructions collectively constrain the motion of the Sierra Nevada-Great Valley block. The third includes constraints from the southern Basin and Range, mainly the mid-Tertiary metamorphic core complexes of the Colorado River corridor and southern Arizona, west of the Sierra Madre Occidental, and extension across the Rio Grande rift north and east of the Sierra Madre Occidental (Table 3). The fourth includes the complex Oligocene to recent strike-slip and extensional displacements of the Mojave region, which connect the Sierran displacement to regions farther south (Figure 5 and Table 4). The fifth includes paleomagnetic and geologic constraints on vertical axis rotations of large crustal blocks, including the Sierra Nevada and Colorado Plateau, as well as small, individual ranges within the central Basin and Range and Mojave regions (Table 5). Lastly, constraints on the large displacements along the San Andreas fault/Gulf of California shear system, and strains and rotations within the Continental Borderlands, including the large clockwise rotation of the Santa Ynez Mountains block, are included in Figure 6 and Table 6.

## Northern Basin and Range.

The extensional kinematics of the northern Basin and Range are dominated by two large-offset normal fault systems, the Snake Range detachment system (78 km of total offset) and the Sevier Desert detachment (40 km of total offset). The Snake Range detachment system affects the Egan, Schell Creek, and Snake Ranges (Figure 2, ranges 6-8). Although the coupling of this system of faults to deep crustal extension has been debated (e.g. Gans and Miller, 1983; Miller et al., 1983; Bartley and Wernicke, 1984, Miller at al., 1999; Lewis et al., 1999), a magnitude of upper crustal extension of 78 ± 10 km, as determined through mapped and restored stratigraphic markers, is not controversial (Gans and Miller, 1983; Bartley and Wernicke, 1984). More controversial is the geometry of the extensional faults in the Sevier Desert basin (between ranges 3 and 4, Figure 2), including the very existence of the Sevier Desert detachment, which is known only from interpretations of seismic reflection profiles and well data (Anders and Christie-Blick, 1994; Wills et al., 2005). The 40 km offset along the Sevier Desert detachment used in this paper is based on restoring Sevier fold-thrust belt structures that are offset by the detachment, and high-angle normal faults in the hanging wall imaged in COCORP and industry seismic reflection lines (Allmendinger et al., 1986; Allmendinger et al., 1995; Coogan and DeCelles, 1996). An opposing view to the large offset kinematics of a shallow detachment suggests that the imaged reflection surface is a composite of aligned features that includes basin-bounding high angel normal faults, a sub-horizontal thrust fault and an evaporite horizon (Anders and Christie-Blick, 1994). According to this interpretation, extension across ranges within and around the Sevier Desert basin could be as little as 10 km (versus 40 km), which would subtract approximately 15% from our overall estimate of extension along the transect.

To the west of the Egan Range area, the remainder of the northern Basin and Range deformation is partitioned into extensional and right-lateral strike-slip offsets, both of which serve to translate the Sierra-Great Valley block away from the interior of North America. The extension (94 km) is accommodated by several systems of steeply tilted normal fault blocks in the western Basin and Range, with individual fault systems accommodating up to 16 km of extension (Figure 2, ranges 13, 19 and 20) (Surpless, 1999; Dilles and Gans, 1995; Smith, 1992) and a number of high-angle, presumably modest-offset normal faults that define the Basin and Range physiography across the central part of the reconstruction path, that we assume have 3 to 4 km of horizontal offset each.

Right lateral shear is accommodated predominantly through northwest trending faults concentrated near the western edge of the northern Basin and Range in the northern Walker Lane Belt (Figure 2, range 18). Right-lateral offset on a series of faults that individually have 5-15 km of offset totals 35-56 km (Faulds et al., 2003; Hardyman et al., 1984). Since the faults strike more westerly than the North American margin, their motion accommodates a component of westward motion of the plate boundary.

Timing of extension in the northern Basin and Range is constrained by a large body of work on the ages of faulted Cenozoic volcanic and sedimentary units and cooling ages of uplifted footwall blocks. For example the early “core complex”-related extension (~35-25 Ma) is seen in coeval faulting and volcanism at 35 Ma in the Egan Range (Gans and Miller, 1983), and $^{40}$Ar/$^{39}$Ar cooling ages indicative of rapid cooling from 30-25 Ma in the western portion of the Northern Snake Range and from 20-15 Ma in the eastern portion of the range (Lee, 1995). AFT cooling ages from the Northern Snake Range indicate 10-13 km of fault slip from 18-14 Ma. Initiation of later “Basin and Range” extension is seen predominantly in the fission-track and helium cooling ages of apatite and zircon. The cooling ages across the width of the extending zone cluster around ~15 Ma (Stockli, 1999), with 18 Ma ages in the footwall of the Snake Range detachment (Miller et al., 1999) (Figure 2, range 6) and Sevier Desert detachment (Stockli et al., 2001), (Canyon Range, Figure 2, range 3).

## Central Basin and Range

The central Basin and Range province is in many respects an ideal location for a province-wide restoration of Basin and Range extension (Snow and Wernicke, 2000 and references therein). A regionally conformable miogeocline, Mesozoic thrust structures and distinctive Tertiary sedimentary deposits tightly limit the extensional history of both the Lake Mead (Figure 2, ranges 22-25) and the Death Valley (Figure 2, ranges 27-34) extensional systems (Wernicke et al., 1988; Wernicke, 1992). Motion of the Sierra Nevada with respect to the Colorado Plateau in this region is primarily constrained by displacements of two distinctive Miocene basins developed early in history of extension of each system (Figure 4).

In the Lake Mead system, restoring numerous proximal landslide breccias at Frenchman Mountain (range 24) to their source areas in the Gold Butte block (range 23) also restores piercing lines defined by the southward truncation Triassic formational boundaries by the basal Tertiary unconformity in both areas. The correlation of these features in the Frenchman Mountain and Gold Butte areas suggests 65±15 km of extension between the two blocks (Figure 4).

In the Death Valley system, Wernicke et al. (1988) initially proposed that the Panamint thrust at Tucki Mountain (Panamint Range, Figure 2, range 28) is the same structure as the Chicago Pass thrust in the Nopah-Resting Springs Range (range 27) and the Wheeler Pass thrust in the Spring Mountains (range 25), suggesting a total of 125±7 km of post-Cretaceous, WNW extension has separated them (Table 2). This offset is strengthened by correlations of additional contractile structures exposed across the Death Valley extensional system (Snow and Wernicke, 1989; Snow, 1992; Snow and Wernicke, 2000), and distinctive middle Miocene sedimentary deposits that occur along the extensional path (Niemi et al., 2001). These include proximal conglomeratic strata of the Eagle Mountain Formation, which were derived almost exclusively from the northeastern margin of the Hunter Mountain batholith in the southern Cottonwood Mountains (Figure 2, range 32). Recognition and correlation of this dismembered early extensional basin, in conjunction with stratigraphic constraints from other Tertiary deposits in the region indicates that its fragmentation occurred mainly from 12-2 Ma (Figure 4). The correlation of these deposits yields a displacement vector of 104 ±7 km oriented N 67° W between the Nopah-Resting Springs Range (Figure 2, range 27) and the Cottonwood Mountains (range 32).

To the ~170 km of extension from these constraints, we add four additional estimates to complete the reconstruction path. In the Lake Mead system, 15 km of extension between the Gold Butte area and the Colorado Plateau (range 23) (Brady et al., 2000), and a maximum of 8 km of extension between the Spring Mountains (range 25) and Frenchman Mountain (range 24)(Wernicke et al., 1988) increases the total displacement of the Spring Mountains relative to the Colorado Plateau to ~88 km. In the Death Valley system, an addition of 9 km of displacement in both the Panamint and Owens Valleys increases the total displacement to ~147 km between the Spring Mountains and the Sierra Nevada.

The sum of all displacements along the path is therefore sums to 235 ±20 km (Table 2), which represents a combination of areal dilation (crustal thinning) and plane strain (strike-slip faulting). Approximately 80% of the elongation is accommodated by vertical thinning, and ~20% by north-south contraction (Wernicke et al., 1988; Snow and Wernicke, 2000). In addition to this path, there are a number of more local offsets that were used to position polygons to the north and south, which are shown on Figure 4 and summarized in Table 2.

### Southern Basin and Range/Rio Grande Rift.

Extension in the southern Basin and Range is almost completely dominated by the formation of large-offset normal faults that form the metamorphic core complexes (Coney, 1980; Spencer and Reynolds, 1989; Dickinson, 2002). The core complexes ring the southwestern margin of the Colorado Plateau (ranges 37-44), and estimates of the total extension they represent are remarkably systematic in magnitude, direction and rate (Table 3). The timing of extension varies in age from 28 Ma to 14 Ma as the extension migrates from southeast to northwest. The migration of extension has been related to a similar migration in volcanism. Both extension and volcanism have been proposed to be a result of the northwestward foundering of the Farralon plate (e.g. Humphreys, 1995; Dickinson, 2002).

In a similar time frame (~26 Ma), volcaniclastic sediments deposited east of the Colorado Plateau in the Rio Grand Rift (Figure 2, location 45) have been interpreted as representing the onset of extension (Chapin and Cather, 1994). Ingersoll (2001) counters that the early sediments are broad volcaniclastic aprons that show no evidence of syndepositional faulting. He places the initiation of rifting slightly later (~21 Ma). Based on initiation of half-graben sedimentation and stratal tilting rapid extension occurred between 17 and 10 Ma (Ingersoll, 2001; Chapin and Cather, 1994). The total magnitude of extension is small and ranges from 6 km in the northern part of the rift to 17 km in the south, consistent with 1.5° clockwise rotation of the Colorado Plateau (Chapin and Cather, 1994, Russell and Snelson, 1994).

Extension within the Rio Grande rift is contiguous with the broad extended region farther south, east of the Sierra Madre Occidental (in Chihuahua), the magnitude of which is poorly understood (Dickinson, 2002). Generally, extension in the Mexican Basin and Range is partitioned both in time and space. Early "core complex" extension is documented in northwestern Mexico (in Sonora), just west of the Sierra Madre Occidental (Nourse et al., 1994; Gans, 1997)(Figure 2). Palinspastic reconstructions over small regions in Sonora suggest cumulative extension of 90% mostly between 26-20 Ma, and more modest extension (10-15%) between 20-17 Ma (Gans, 1997). Limited crustal extension is also documented east of the Sierra Madre Occidental during the same time period (Dickinson, 2002). Major extension occurred in both Chihuahua (Henry and Aranda-Gomez, 2000, Dickinson, 2002) and Sonora Mexico (e.g. Stock and Hodges, 1989; Henry, 1989; Lee et al., 1996) from ~12-6 Ma as a prelude to the opening of the Gulf of California at 6 Ma (Oskin et al., 2001). During the 12-6 Ma interval, very small magnitude, east-west "Basin and Range" extension affected Arizona (Spencer and Reynolds, 1989, Spencer et al., 1995).

## Mojave Region

Cenozoic deformation of the Mojave region occurred in two main stages. Deformation began in the late Oligocene/ early Miocene with the formation of large-offset normal faults and associated core complexes (Glazner et al., 1989; Dokka,1989; Walker et al., 1990). Extension in the Mojave region (Figure 2, range 41 and Figure 4) may be linked to core complex extension in the southern Basin and Range corridor (Figure 2, ranges 38, 44) through a diffuse transfer zone that involves both rotation and strike slip faulting (Bartley and Glazner, 1991, Martin et al., 1993). The magnitude of extension is determined through alignment of pre-extensional markers that include facies trends in Paleozoic strata, a unique gabbro-granite complex and late Jurassic dikes, indicating a total of 40-70 km of offset (Glazner et al., 1989; Walker et al., 1990; Martin et al., 1993). Extension began in synchronism with the eruption and emplacement of 24-23 Ma igneous rocks (Walker et al., 1995) and is capped by the flat lying, 18.5 Ma Peach Springs Tuff (Glazner et al., 2002). The fraction of the Mojave Desert region that was affected by mid-Tertiary extension is controversial (e.g. Dokka, 1989; Glazner et al., 2002). Glazner et al. (2002) propose that only a small region north of Barstow (Figure 2, range 41) was affected by the early extension, with the southern boundary of this extensional domain linked to core complex extension to the southeast through diffuse right-lateral shear. The northern boundary of the extensional domain is more problematic, however regional kinematic compatibility requires a northern transfer zone that links Mojave extension to similar age extension to the north or west. Rotation of the Tehachapi Mountains and/or extension in the southern San Joaquin Valley may represent the northern portion of this system (McWilliams and Li, 1985; Plescia and Calderone, 1986; Tennyson, 1989; Goodman and Malin; 1992; Glazner et al., 2002).

Following this early phase of extensional deformation, a system of right- and left-lateral strike-slip faults characteristic of those active today was established, dominated by distributed right-lateral shear along a series of northwest-striking faults Figure 5). The total accumulated shear across the Mojave, as documented by field studies is 53 km ± 6 km (Table 4). The timing of right-lateral shear is not constrained. Motion on the faults is inferred to be post-10 Ma based on strain compatibility with deformation directly north and south (Tables 2 and 5).

**Vertical Axis Rotations East of the San Andreas Fault.**

There are two zones of vertical-axis rotation east of the San Andreas fault, the Eastern Transverse Ranges located immediately south of the Mojave block and the northeastern Mojave rotational block (Carter et al., 1987; Schermer et al., 1996; Dickinson, 1996)(Figure 5)(Table 4).

The Eastern Transverse Ranges include a series of structural panels separated by east-west oriented, left-lateral faults (Dickinson, 1996). Paleomagnetic studies show that 10 ± 2 Ma rocks within this zone record the entire 45° rotation (Carter et al., 1987), while 4.5 Ma volcanic rocks are unrotated (Richard, 1993). These constraints imply that all of the rotation and most of the right-lateral strike slip motion in the Mojave region immediately to the north are ~10 Ma and younger.

The northeastern corner of the Mojave region is another area of pronounced clockwise rotation. Schermer et al. (1996) proposed that the northeastern Mojave underwent 23° of rotation accompanied by 5 km of left lateral slip on faults within the rotating region and 15° of "rigid body" rotation. Total right lateral shear predicted by this model is 33 km.

**San Andreas System and Areas to the West.**

Deformation west of the San Andreas Fault is defined by four first-order constraints (Figure 6)(Table 6). The first is motion on the San Andreas fault itself, which is tightly constrained in central California at 315 ± 10 km by restoring the Pinnacles volcanics west of the fault to the Neenach volcanics to the east of it (Matthews, 1979, Graham et al., 1989; Dickinson, 1996). The offset volcanics were extruded from 22 to 24 Ma, but tentatively correlative late Miocene strata (7-8 Ma) are apparently offset 255 km (Graham, 1989; Dickinson, 1996).

The second constraint is the ~110° degree clockwise rotation of major fault-bounded blocks in the western Transverse Ranges (Hornafius et al., 1986; Luyendyk, 1991). Because of the length and structural integrity of these blocks (in particular, the Santa Ynez Mountains), this rotation requires a coast-parallel displacement of ~270 km (Hornafius et al., 1986).

The shear and rotation of these blocks is confirmed by the third major constraint, reconstruction of now-scattered outcrops of the distinctive Eocene Poway Group. Exposures along the Channel Islands were rifted away from counterparts in southernmost California, which are in turn offset from their source area in northern Sonora, Mexico by the southern San Andreas fault system (Abbott and Smith, 1989). Rifting and rotation of the western Transverse Ranges away from the Peninsular Ranges formed the strongly attenuated crust of the Continental Borderlands on their trailing edge. The magnitude of this extension is proposed to be ~250 km based on seismic reflection data delineating the geometry of extensional fault systems and correlation of "mega key-beds" or lithotectonic belts (forearc basin sediment, Franciscan subduction complex)(Crouch and Suppe, 1993; Bohannon and Geist, 1998).

The final first-order constraint is the closing of the Gulf of California. Although offset of the Poway Group suggests roughly 250 km of displacement, recognition of correlative pyroclastic flows on Isla Tiburon and near Puertecitos on the Baja Peninsula dated at 12.6 and 6.3 Ma constrains the full transfer of Baja California to the Pacific plate to have occurred no earlier than ~6 Ma, with 255 ± 10 km of displacement along the plate boundary since then (Oskin et al., 2001).

## DISCUSSION

The exercise of developing a self-consistent, strain-compatible model has raised a number of issues that are difficult to resolve satisfactorily in the reconstruction and require further investigation. The most apparent (among many!) are 1) the need for middle to late Miocene right-lateral shear in the eastern Mojave region to "make room" for the northerly motion of the Sierra Nevada determined from the central and northern Basin and Range reconstruction paths; 2) the need for large amounts of relatively young extension in northern Mexico both east and west of the Sierra Madre Occidental to reconcile core complex extension in Arizona and the late Miocene/Pliocene opening of the Gulf of California, and 3) generally large amounts of Miocene/Pliocene shortening and extension in the Transverse Ranges, Coast Ranges and Borderlands provinces, which arise from the need to reconcile San Andreas offset with the position of oceanic crust offshore, differences in the age of extension north and south of the Garlock fault and large clockwise rotation of the Santa Ynez Mountains block.

### Eastern Mojave region

The eastern California shear zone (ECSZ)/Walker Lane belt is a ~120 km-wide zone of right-lateral, intraplate shear east of the Sierra Nevada and San Andreas fault. Geodetically this shear zone accommodates up to 25% of the Pacific-North America relative plate motion (Bennett et al., 2003; McClusky et al., 2001, Miller et al., 2000, Sauber et al., 1994). Geologic estimates of displacements vary along the north-south extent of the ECSZ. Proposed net displacement along the ECSZ (oriented ~N 20 W) varies from 65 km in the Mojave region (Dokka and Travis, 1990) to 133 km in the central Basin and Range (Snow and Wernicke, 2000; Wernicke et al., 1988). In the northern Walker Lane region, shear estimates range from 30-54 km (Faulds et al., 2003; Hardyman et al., 1984), plus an additional component of NW-directed extension due to a change in extension direction in the northern Basin and Range from EW in the east to NW-SE in the west.

One of the goals of this study was to develop a kinematically consistent model of the ECSZ that fits within the errors provided by both local and regional studies. We found 100 km ± 10 km right-lateral shear oriented N25°W was compatible with data in both the northern and central Basin and Range. In the Mojave region of the ECSZ, however, available data suggests no more than 53 ± 6 km of right-lateral shear oriented N25°W, about half of what is required to the north. Kinematic compatibility with the magnitude of deformation north of the Garlock fault requires ~100 km of right lateral shear though the Mojave region, with the majority of additional shear located on the eastern edge of the shear zone during its early (12-6 Ma) history (Figure 5). The 27 and 45 km of right lateral offset along the Bristol

Mountains/Granite Mountain and southern Death Valley fault zones is significantly greater than previous estimates (0-10 km and 20 km respectively), but solid piercing points that limit the net offset are scarce and debatable (Howard and Miller, 1992; Dokka and Travis, 1990; Davis, 1977). Less forgiving are the 11-13 km model offsets on the Camp Rock, Gravel Hills and Harper Lake fault systems, where current estimates suggest no more than 3 km of offset on any of these faults (Dibblee, 1964; Oskin et al., 2004: M. Strane, Pers. Comm., 2005). The difference between the model and data requires that the slip discrepancy must be must be taken up on other faults (most likely to the east) in the Mojave shear system. Although the details concerning both timing and distribution of shear within the ECSZ will continue to evolve with time, the strength of the central Basin and Range offsets combined with kinematic compatibility constraints require re-evaluation of geologic evidence for total magnitude of right-lateral shear through the Mojave. Therefore we have modeled many of the faults in the Mojave with greater net offset than suggested by offset markers. From the model slip amounts shown on Figure 5, we obtain 100 km of right-lateral shear oriented N25°W since 12 Ma, at a long-term rate of 8.3 ± 1 mm/yr. We suggest that the discrepancy may be due to penetrative shear in the largely granitic crust between the strike-slip faults.

Dokka and Travis (1990) proposed that the ECSZ accommodated 9-14 % of total predicted relative motion between plates if shear initiated at 10 Ma. The model of ECSZ deformation that we propose here suggests that ECSZ deformation is approximately 28% of San Andreas motion averaged since 12 Ma and 15% of total plate motion since 16 Ma.

## Arizona/Mexican Basin and Range

The geographic region that has the fewest local kinematic constraints is Sonora/ Chihuahua Mexico. However, the kinematics of Baja California, based on plate tectonic reconstructions (Atwater and Stock, 1998), is an especially powerful constraint on intraplate deformation in this region. The constraint arises from the simple fact that oceanic and continental lithosphere cannot occupy the same surface area at the same time (Atwater and Stock, 1998) (Figure 6b). The plate tectonic constraint suggests ~330 ± 50 km of extension between 6 and 24 Ma, because after restoring the offset across the Gulf of California (Oskin et al., 2001), this is the total overlap between continent and ocean. In concert with strong NE-SW extension in Arizona, we suggest similar magnitudes of extension (44 and 86 km) occurred from 16-24 Ma and was oriented N 50-60 E (making room for the brown and green curves in Figure 6b). We show another pulse from 12-8 Ma oriented N65-78W, reflecting the growing influence of the Pacific plate's northerly motion on intraplate deformation, as appears to be the case to the north.

However. restoring 330 km of extension, particularly the northwesterly extension in the window of time from 16-8 Ma, opens up an unacceptable, northeast-trending gap in southern Arizona and northern Sonora. This gap is a result of differences in both magnitude and timing of extension between southern Arizona and northern Sonora. Large magnitude "core complex" extension in southern Arizona initiates at approximately 28 Ma and wanes from 16-14 Ma (Table 3). Significant extension in Sonora occurs over a similar time range (Nourse et al., 1994; Gans, 1997). However at ~12 Ma significant extension is recorded in both the Gulf extensional province west of the Sierra Madre Occidental (e.g. Stock and Hodges, 1989; Henry, 1989; Lee et al., 1996) and east of the Sierra Madre Occidental (Henry and Aranda-Gomez, 2000), while only minimal magnitudes of east-west extension is recorded in southern Arizona. This problem is similar to that arising from the difference in timing of extension north of the Colorado River extensional corridor between the Mojave Desert and central Basin and Range. Here, the Garlock fault accommodates different amounts of extension, not only from 10 Ma to present (Davis and Burchfiel, 1973), but potentially throughout the history of extension in the region (24-0 Ma). Although the difference in timing and magnitude of extension between the Mojave region and the southern Arizona Basin and Range, versus the Mexican Basin and Range in Sonora and Chihuahua is generally recognized (e.g. Henry and Aranda-Gomez, 2000, Dickinson, 2002), the geometry and genetic relationship of the transfer system that must separate them is problematic.

In the model presented here, the amount of extension in the Mexican Basin and Range is partitioned between the extending regions east (~134 km) and west (~180 km) of the unstrained Sierra Madre Occidental block. Although both regions display numerous extensional structures, the exact magnitude of extension is unknown. Because of the difference in post-16 Ma extension in Chihuahua and the Rio Grande rift (90 and 20 km, respectively) after ~16 Ma, the model includes a zone of right-lateral shear that extends through southeastern Arizona between the two provinces. The existence of this shear zone is unlikely, leaving two possible solutions. The first is that extension systematically increases from the Rio Grande rift to Chihuahua Mexico due to clockwise rotation of the Sierra Madre Occidental (rotation would need to be greater than the 1.5 ° rotational opening of the Rio Grande rift). Another solution would be partitioning a much greater magnitude of extension in the Gulf extensional province (~270-300 km), but this is thus far not supported by mapping in the region (Henry and Aranda-Gomez, 2000). Most likely some combination of these factors is necessary to match the first order geologic constraints of the region

## Areas West of the San Andreas fault.

Based on the timing and magnitude of displacement on a few fault systems (San Andreas, northern Gulf of California, Mojave, central Basin and Range, and the Santa Ynez Mountains), continental basins must open (creation of white spaces in the movie suggesting pulses of extension) and close (closing of spaces or overlap of polygons suggesting pulses of contraction) from 24 to 0 Ma. Even at this large and relatively simplified scale, extension and contraction are spatially and temporally complex throughout the region west of the San Andreas fault, and we might expect even greater complexities in timing and magnitude at a more detailed level. The following discussion highlights the magnitudes of displacement and summarize data that either support or conflict with the model displacements.

**Transverse Ranges.** The clockwise rotation of the Western Transverse Ranges (Hornafius et al., 1986; Luyendyk, 1991) suggests regions of extension and subsequent compression both north and south of the rotating Santa Ynez Mountains block (Figure 2, range 50). The magnitude of predicted extension and contraction (oriented ~N-S) is as great as 130 km to the north of the western side of the block from ~12 Ma to present. Motion of Baja California northward from 6 Ma to present suggests as much as 90 km of shortening in the southern Transverse Ranges (Santa Ynez and San Gabriel Mountains blocks). Transpressive motion involving the San Gabriel Mountains, San Bernardino Mountains and Mojave blocks implies ~40 km of N-S shortening immediately north of the Peninsular Ranges block. Balanced cross sections through the San Emigdio, Santa Ynez and San Gabriel Ranges indicate 53 km of shortening since 3 Ma (Namson and Davis, 1988a). Although the shortening estimate is strongly dependent on the details of how the Santa Ynez and Peninsular Ranges/Baja California blocks move, the reconstruction presented here suggests ~ 60 km of N-S shortening at the longitude of the eastern Santa Ynez Mountains block since 6 Ma. As suggested by Namson and Davis (1988a), shortening of this magnitude in the upper mantle lithosphere is supported by a large volume of high-velocity material imaged tomographically beneath the region (e.g. Humphreys et al., 1984).

**Coast Ranges.** Differences in the timing of extension within the Mojave and Basin and Range north and south of the Garlock fault, in conjunction with plate tectonic constraints on the westernmost limit of the North America continental edge (Atwater and Stock, 1998) indicate a period of extension (20-16 Ma) and subsequent compression (14-0) to the west of the Sierra/ Great Valley block. Approximately 80 km of core-complex extension south of the Garlock fault occurred prior to significant extension in the central Basin and Range. In order to maintain a quasi-linear ocean-continent boundary, a zone of extension, roughly equal in magnitude to the core-complex extension, is required north of the Garlock fault and west of the Sierra Nevada/ Great Valley block, most visible in the reconstruction at 16 Ma. As extension evolves in the central Basin and Range, this same zone undergoes contraction to maintain the quasi-linear plate boundary suggested by the extant distribution of oceanic crust from 16 Ma to present.

The Neogene tectonic and volcanic history from the Great Valley to the edge of the continent is broadly consistent with the model (data summarized in Tennyson, 1989). The model and geologic data are difficult to compare quantitatively because there are no obvious normal faults with measurable offsets. Development of local non-marine basins and eroded highs, followed by significant subsidence at ~16 – 18 Ma and the development of the relatively deep marine Monterey basin strongly suggests an extensional event. Rotation of the Tehachapi Mountains and/or extension in the southern San Joaquin Valley (McWilliams and Li, 1985; Plescia and Calderone, 1986; Tennyson, 1989; Goodman and Malin; 1992) may be indicative of this extension but may represent far less than the ~80 km predicted by the model.

The subsequent compression in the Coast Ranges is more quantifiable and appears to be significantly less than that suggested by the model. Estimates of compression in the Coast Ranges east and west of the San Andreas fault range from 20 km to 48 km (Page et al., 1998; Namson and Davis, 1990; 1988b; Page et al., 1978) with all of the known shortening post-10 Ma, and most of it post 4-Ma (Page et al., 1998; Namson and Davis, 1990). Therefore the model predicts an additional 32-50 km of shortening prior to 10 Ma, for which there is (thus far) no evidence in the Coast Ranges.

## Uncertainties in the Reconstruction.

Statistically rigorous uncertainties are notoriously difficult to quantify in geological reconstructions, largely because estimates of geologic offset do not have Gaussian or other standard probability distribution functions. The condition of strain compatibility or "no overlap" sets a hard limit on the displacement estimate but does not distinguish higher or lower probability of any given position within those limits. Hence the variance of any given estimate cannot be rigorously quantified.

In map view, any given displacement estimate will have an irregularly shaped uncertainty region. Under the assumption of a uniform probability distribution within these uncertainty regions, Wernicke et al. (1988) used a Monte Carlo method to estimate the total uncertainty on the sum of displacement vectors for a path across the central Basin and Range. This method repeatedly summed randomly selected vectors from each uncertainty region to generate a probability distribution for the net offset. The contour that excluded the outermost 5% of the model runs was taken as an estimate of two standard deviations of the measurement. The estimate of total Sierran motion thus derived was 247 ± 56 km S75 ± 12°E, and therefore a reasonable estimate of the standard deviation would be 28 km. For this same estimate, the square root of the sum of the squares for individual vectors (in the direction of displacement, using values from Table 1 and Figure 10 of Wernicke et al., 1988) is only 15 km. This is perhaps not surprising because the Monte Carlo approach does not place greater weight on values near the center of the uncertainty polygon than on values at the edges.

Our revised displacement estimate for the central Basin and Range, 235 ± 20 km, is similar to that of Wernicke et al. (1988) if one considers the 20 km figure as a crude estimate of the standard deviation (1-sigma). However, given the results from Wernicke et al. (1988), the real error may scale upward by as much as a factor of two, depending on the degree to which our “best estimate” is more probable than values at the extremes. Thus as a rule of thumb, the uncertainty in position of any given range or set of ranges at any given time is on the order of 20-40 km at one standard deviation.

Because the reconstruction involves temporal information (which is also uncertain), the problem of rigorously estimating errors becomes even more difficult, and is clearly beyond the scope of this paper. Even though temporal information adds to the uncertainty of position at any given time, the self-consistency of the reconstruction mitigates these uncertainties to a substantial degree.

## EVOLUTION OF THE REGIONAL VELOCITY FIELD

Tracking the restored positions of the ranges from the palinspastic maps, we have created “instantaneous” velocity fields based on 2 Myr averages from 0 to 18 Ma, and 6 Myr averages from 18 to 36 Ma. These “paleogeodetic” velocity fields depict how deformation has evolved in space and time across the plate boundary deformation zone (Figure 7a-g).

Figures 7f and g (30-18 Ma) illustrate the collapse of the Basin and Range away from the stable Colorado Plateau through the formation of metamorphic core complexes, at a time of active ignimbrite volcanism and Pacific-Farallon convergence. Extension initiated first in the northern Basin and Range (NBR) and then in the southern Basin and Range (SBR). This pulse of large magnitude extension migrated south and north respectively until it converged in the central Basin and Range (CBR) at ~16 Ma. Figure 7e (14-16 Ma) emphasizes the large extensional strains in the CBR especially with respect to the concurrent faulting to the north and south. The 14-16 Ma time slice also shows the impact of the evolving plate boundary on the North American continent as right lateral shear is accommodated through the rotation of the Western Transverse Ranges and accompanying shear and extension. The 10-12 Ma time slice (Figure 7d) illustrates the uniform (systematically increasing) strain in the NBR and in contrast the westward migrating extension in the CBR. Significant extension is also necessary in the Mexican Basin and Range due to plate boundary constraints. It is during this time period that right-lateral shear migrates farther inboard into the continent through the development of the ECSZ. South of the Garlock fault the shear is oriented nearly parallel to the plate boundary (N25°W). North of the Garlock fault the shear plus extension creates a more oblique orientation of shear (~N67°W). From 6-8 Ma this same pattern of intracontinental right-lateral shear strengthens with shear partitioned differently south of the Garlock fault than in the CBR and NBR portions of the ECSZ. In the Mexican Basin and Range deformation wanes and extension and right lateral shear become concentrated in the proto-Gulf of California

The differences in the velocity fields from the 2-4 Ma average to the 0-2 Ma average is most likely a function limitations in the data, rather than a significant slowing in the rate of deformation over the last 2 Myr (i.e. the Mojave region). Within the model, the lack of timing constraints for right-lateral faults through the Mojave means that the rate of deformation there becomes a function of the rate of deformation to the north and south. North of the Garlock fault, large magnitudes (104 km) of oblique extension are focused predominately from 11-3 Ma (Niemi et al., 2001; Snow and Wernicke, 2000; Snow and Lux, 1999). South of the Mojave, the timing of deformation is partially bracketed by the age of rotation of the Eastern Transverse Ranges (as mentioned earlier, ~10 Ma rocks record the entire 45° of rotation whereas ~4 Ma rocks indicate no rotation; Carter et al., 1987; Richard, 1993). These timing constraints suggest most of the deformational shear in the Mojave occurred between 10 and 2 Ma. However, the total displacement across the eastern California shear zone (100 km ± 10 km) averaged over the last 12 Myr suggests a long-term rate of 8.3 ± 1 mm/yr. This rate is similar to or slightly less than the 8-12 mm/yr rate suggested by geodetic studies (McClusky et al., 2001, Miller et al., 2000, Sauber et al., 1994, Savage, 1990).

Another way to look at the evolution of the velocity field and provide a direct comparison between geologic data and geodynamical model results is by mapping the paths that individual ranges take over the deformational interval of interest (Figure 8). Note that the bend in the path of the Pacific plate does not appear to be related to changes in the paths the Sierra Nevada with respect to the Colorado Plateau or changes in the paths of individual ranges within the continent. The most significant continental change in direction occurs at 12 Ma. Because the plate constraints do not require the bend to occur at that time (it is only a function of the times at which magnetic anomalies constrain the position), it is possible within the uncertainties of both the plate reconstruction and geological reconstruction (Atwater and Stock, 1998; Wernicke and Snow, 1998) that these events more closely correlate. As stated previously the timing of development of right-lateral shear depends on the orientation and timing of early extension in the Death Valley region, which if relatively minor prior to 11 Ma would point toward a later time of onset of right-lateral shear inboard of the Sierra Nevada. The distribution of north-northwest shear through the Mojave is kinematically linked to the northwesterly motion of the Sierra Nevada/ Great Valley block, in turn requiring at least some amount of right lateral shear within the Mojave region between 12 and 8 Ma.

## CONCLUSIONS

Although orogen-scale reconstructions of the Basin and Range will continue to evolve with time and adjust as more data is acquired, the exercise in kinematic compatibility we present here highlights what we understand and more importantly what we still do not understand regarding the evolution of the plate boundary.

Results that are robust and highlight what we do understand include: 1) 235 ±20 km of extension oriented N78°W in both the northern (50% extension) and central (200% extension) parts of the province. An important implication of the model is that any significant change in extension amount in a portion of the region (i.e a range on the path between the Colorado Plateau and the Sierra Nevada) must be evaluated in light of how that change affects co-evolving regions to the north and south. 2) A significant portion of boundary-parallel shear (in contrast to earlier extension) jumped into the continent at ~10-12 Ma and once established, appears to have migrated westward with time. 3) The magnitude of slip on the ECSZ appears to be 100 ±10 km, although the exact structures that accommodate this shear in the Mojave, or how much of the relative motion is accommodated by distributed shear, is not known.

Problems with the current reconstructions are highlighted by large gaps in the model. These zones emphasize areas where more work is needed in refining our ideas about how intraplate deformation is transferred and accommodated through time. Salient aspects of the model that we do not understand include: 1) Compatibility between timing of extension north and south of the Garlock fault and a smooth NNW-trending continental edge as implied by plate tectonic reconstructions. To maintain a relatively smooth continental edge with different periods of extension across the Garlock fault, a triangular window of significant extension (>50 km) (24-16 Ma) followed by an equal amount of shortening (14-0 Ma) would have occurred in the Coast Range/ Great Valley region. While known geology supports extension and subsequent compression in these time windows, the magnitude is ~25 % of what is needed. 2) Differences in magnitude and timing of extension between southern Arizona and northern Sonora, Mexico require a transfer zone or large lateral displacement gradient. The model displays this zone as a gap that opens up (going backward with time) between the two provinces. Timing and magnitude of extension in the Sonora region was constrained only by plate motions to the west and broad assumptions as to similarities in timing and direction with areas to the north. Data detailing the magnitude, timing and direction of extension through the Mexican Basin and Range is necessary to resolve this problem.

## REFERENCES

Abbott, P. L., and Smith, T. E., 1989, Sonora Mexico, source for the Eocene Poway conglomerate of southern California: Geology, v. 17, p. 329-332.

Allmendinger, R. W., Farmer, H., Hauser, E. C., Sharp, J., and Von Tish, D., Oliver, J., and Kaufman, S., 1986, Phanerozoic tectonics of the Basin and Range–Colorado Plateau transition from COCORP data and geologic data, in Barazangi, M. a. B., L., ed., Reflection seismology: The continental crust, American Geophysical Union Geodynamics Series, p. 257-268.

Allmendinger, R.W., Royse, F., Anders, M.H., Christie-Blick, N., and Wills, S., 1995, Is the Sevier Desert reflection of west-central Utah a normal fault?; discussion and reply: Geology 1995 23: 669-670.

Anders, M. H., and Christie-Blick, N., 1994, Is the Sevier Desert reflection of west-central Utah a normal fault?: Geology v. 22, p. 771–774.

Atwater, T., 1970, Implications of plate tectonics for the Cenozoic tectonic evolution of western North America: Geological Society of America Bulletin, v. 81, p. 3513-3536.

Atwater, T., and Stock, J., 1998, Pacific-North America Plate tectonics of the Neogene Southwestern United States; an update, in Ernst, W. G., and Nelson, C. A., eds., Integrated Earth and environmental evolution of the Southwestern United States; the Clarence A. Hall, Jr. volume: Columbia, Bellwether Publishing, p. 393-420.

Axen, G.J., Wernicke, B.P., Skelly, M.J., and Taylor, W.J., 1990, Mesozoic and Cenozoic tectonics of the Sevier thrust belt in the Virgin River Valley area, southern Nevada: in Wernicke, B., ed., Basin and Range extensional tectonics near the latitude of Las Vegas, Nevada, Geological Society of America Memoir 176, p. 123-153.

Ballard, S. N., 1990, The Structural geology of the Little Maria Mountains, Riverside County, California [Ph.D. thesis]: University of California, 206 p.

Bartley, J. M., Wernicke, B.P., 1984, The Snake Range decollement interpreted as a major extensional shear zone: Tectonics, v. 3, p. 647-657.

Bartley, J.M., and Glazner, A.F., 1991, En echelon Miocene rifting in the southwestern United States and model for vertical-axis rotation in continental extension: Geology, v. 19, p. 1165–1168.

Bassett, A. M., and Kupfer, D. H., 1964, A geologic reconnaissance in the southeastern Mojave Desert, California: Special Report - California Division of Mines and Geology, v. 83, p. 1-43.

Bennett R. A., Davis J. L, and Wernicke B. P, 1999, Present-day pattern of Cordilleran deformation in the western United States Geology, v. 27 p. 371-374.

Bennett R. A., Wernicke B.P, Niemi N. A., Friedrich, A.M., and Davis J.L., 2003, Contemporary strain rates in the northern Basin and Range province from GPS data, Tectonics v. 22 p. 1008.

Bogen, N. L., and Schweickert, R. A., 1985, Magnitude of crustal extension across the northern Basin and Range Province; constraints from paleomagnetism: Earth and Planetary Science Letters, v. 75, no. 1, p. 93-100.

Bohannon, R. G., and Geist, E., 1998, Upper crustal structure and Neogene tectonic development of the California continental borderland: Geological Society of America Bulletin, v. 110, p. 779-800.

Brady, R., Wernicke, B., and Fryxell, J., 2000, Kinematic evolution of a large-offset continental normal fault system, South Virgin Mountains, Nevada: Geological Society of America Bulletin, v.112, p.1375-1397.

Braun, J.,and Pauselli, C., 2004, Tectonic evolution of the Lachlan Fold Belt, southeastern Australia: constraints from coupled numerical models of crustal deformation and surface erosion driven by subduction of the underlying mantle : Physics of the Earth and Planetary Interiors, v. 141, p. 281-301

Burchfiel, B. C., Hodges, K.V., and Royden, L.H., 1987, Geology of Panamint Valley-Saline Valley pull apart system, California: Palinspastic evidence for low-angle geometry of a Neogene range-bounding fault: Journal of Geophysical Research, v. 92, p. 10422-10426.

Carr, W. J., Byers, F. M., Jr., and Orkild, P. P., 1986, Stratigraphic and volcano-tectonic relations of Crater Flat Tuff and some older volcanic units, Nye County, Nevada, U. S. Geological Survey Professional Paper: Reston, VA, United States, U. S. Geological Survey, 28 p.

Carter, J. N., Luyendyk, B. P., and Terres, R. R., 1987, Neogene clockwise tectonic rotation of the eastern Transverse Ranges, California, suggested by paleomagnetic vectors: Geological Society of America Bulletin, v. 98,p. 199-206.

Cemen, I., Wright, L. A., Drake, R. E., and Johnson, F. C., 1985, Cenozoic sedimentation and sequence of deformational events at the southeastern end of Furnace Creek strike-slip fault-zone, Death Valley region, California, in Biddle Kevin, T., and Christie Blick, N., eds., Strike-slip deformation, basin formation, and sedimentation.: Special Publication - Society of Economic Paleontologists and Mineralogists: Tulsa, OK, United States, SEPM (Society for Sedimentary Geology), p. 127-139.

Chapin, C. E., and Cather, S.M., 1994, Tectonic setting of the axial basins of the northern and central Rio Grande rift, in Keller, G. R., and Cather, S.M., ed., Basins of the Rio Grande rift: Structure, Stratigraphy, and Tectonic setting: Geological Society of America Special Paper 291, p. 5-25.

Coogan, J. C., and DeCelles, P.G., 1996, Seismic architecture of the Sevier Desert detachment basin: evidence for large-scale regional extension: Geology, v. 24, p. 933-936.

Coogan, J. C., DeCelles, P. G., Mitra, G., and Sussman, A. J., 1995, New regional balanced cross-section across the Sevier Desert region and central Utah thrust belt: Geological Society of America Abstracts with Programs, v. 27, no.4, p. 7.

Coney, P.J., 1980, Cordillera metamorphic core complexes: An overview, in Crittended, M.D., Coney, P.J., and Davis, G.H., eds., Cordilleran metamorphic core complexes, Geological Society of America Memoir 153, p. 7-31.

Crouch, J. K., and Suppe, J., 1993, Late Cenozoic tectonic evolution of the Los Angeles basin and inner California borderland: A model for core-complex–like crustal extension: Geological Society of America Bulletin, v. 105, p. 1415-1434.

Davis, G.A., 1977, Limitations on displacement and southeastward extent of the Death Valley fault zone, California: Short contributions to California Geology, Special Report 129, p. 27-33.

Davis, G.A., and Burchfiel, B.C., 1973, Garlock Fault: an intracontinental transform structure, southern California: Geological Society of America Bulletin, v. 84, p. 1407-1422.

Davis, G. A., and Lister, G. S., 1988, Detachment faulting in continental extension; perspectives from the Southwestern U.S. Cordillera, in Clark Sydney, P., Jr., Burchfiel, B. C., and Suppe, J., eds., Processes in continental lithospheric deformation.: Special Paper 218, p. 133-159.

Davy, P., Guerin, G., and Brun, J.-P., 1989, Thermal constraints on the tectonic evolution of a metamorphic core complex (Santa Catalina Mountains), Arizona: Earth and Planetary Science Letters, v. 94, p. 425-440.

Dibblee, T.W., Jr., 1964, Geologic map of the Ord Mountains quadrangle, San Bernardino County, California, U.S. Geological Survey Miscellaneous Geologic Investigations Map I-427.

Dibblee, T.W., Jr, 1968, Geologic map of the Twentynine Palms quadrangle, San Bernardino and Riverside counties, California: U.S., Geological Survey Miscellaneous Geologic Investigations Map I-561.

Dibblee, T.W., Jr., 1982, Regional Geology of the Transverse Ranges Province of Southern California, in Fife, D., ed., Geology and Mineral Wealth of the California Transverse Ranges: Santa Ana, California, South Coast Geological Society, Inc, p. 7-26.

Dickinson, W.R., 1991, Tectonic setting of faulted Tertiary strata associated with the Catalina core complex in southern Arizona: Geological Society of America Special Paper 264, p. 106.

Dickinson, W. R., 1996, Kinematics of transrotational tectonism in the California Transverse Ranges and its contribution to cumulative slip along the San Andreas transform fault system, Geological Society of America Special Paper 305, p. 46.

Dickinson, W. R., and Wernicke, B.P., 1997, Reconciliation of San Andreas slip discrepancy by a combination of interior basin-range extension and transrotation near the coast: Geology, v. 25, p. 663-665.

Dickinson, W., 2002, The Basin and Range Province as a composite extensional domain: International Geology Review, v. 44, no. 1, p. 1-38.

Dilles, J. H., Gans, P. B., 1995, The chronology of Cenozoic volcanism and deformation in the Yerington area, western Basin-and-Range and Walker Lane: Geological Society of America Bulletin, v. 107, p. 474-486.

Dillon, J.T., 1975, Geology of the Chocolate and Cargo Muchacho Mountains, southeasternmost California [Ph.D. thesis], University of California, Santa Barbara.

Dokka, R. K., 1983, Displacements on Late Cenozoic strike-slip faults of the central Mojave Desert, California: Geology, v. 11, p. 305-308.

Dokka, R.K., 1989, The Mojave extensional belt of southern California: Tectonics, v. 8, p. 363-390.

Dokka, R. K., and Travis, C. J., 1990, Late Cenozoic strike-slip faulting in the Mojave Desert, California: Tectonics, v. 9, no. 2, p. 311-340.

Dokka, R. K., Ross, T. M., and Lu, G., 1998, The Trans Mojave-Sierran shear zone and its role in early Miocene collapse of southwestern North America in: Continental transpressional and transtensional tectonics: Geological Society Special Publications 135, p. 183-202.

Duebendorfer, E. M. and Black, R.A., 1992, The kinematic role of transverse structures in continental extension: An example from the Las Vegas Valley shear zone, Nevada: Geology, v. 20, p. 1107-1110.

Duebendorfer, E. M., Beard, L. S., and Smith, E. I., 1998, Restoration of Tertiary deformation in the Lake Mead region, southern Nevada; the role of strike-slip transfer faults, in Faulds James, E., and Stewart John, H., eds., Accommodation zones and transfer zones; the regional segmentation of the Basin and Range Province.: Special Paper 323, p. 127-148.

England, P., Houseman, G. 1986, Finite strain calculations of continental deformation .2. Comparison with the India-Asia collision zone. Journal of Geophysical Research, v., 91, p.3664-3676.

England, P. and McKenzie, D., 1982, A this viscous sheet model for continental deformation: Geophysical Journal of the Royal Astronomical Society, v. 70, p. 1982.

Faulds, J. E., Henry, Christopher D., and Hinz, Nicholas H., 2003, Kinematics and cumulative displacement across the northern Walker Lane, an incipient transform fault, northwest Nevada and northeast California: Geological Society of America Abstracts with Programs, v. 36, no. 6, p. 125-12.

Fayon, A.K., Peacock, S.M., Stump, E., and Reynolds Stephen, J., 2000, Fission track analysis of the footwall of the Catalina deatchment fault, Arizona: Tectonic denudation, magmatism and erosion: Journal of Geophysical Research, v. 105, p. 11047-11062.

Fitzgerald, P. G., Fryxell, J.E. and Wernicke, B.P., 1991, Miocene crustal extension and uplift in southeastern Nevada: Constraints from apatite fission track analysis.: Geology, v. 19, p. 1013-1016.

Flesch, L. M., Holt, W.E., Haines, A. J., and Shen-Tu, B., 2000, Dynamics of the Pacific-North American plate boundary in the western United States, Science v. 287, p. 834-836.

Fletcher, J. M., Bartley, J. M., Martin, M. W., Glazner, A. F., and Walker, J. D., 1995, Large-magnitude continental extension; an example from the central Mojave metamorphic core complex: Geological Society of America Bulletin, v. 107, no. 12, p. 1468-1483.

Foster, D. A., Gleadow, A.J.W., Reynolds, S.J., and Fitzgerald, P.G., 1993, Denudation of metamorphic core complexes and the reconstruction of the Transition Zone, west-central Arizona; Constraints from apatite fission track thermochronology: Journal of Geophysical Research, v. 98, p. 2167-2185.

Fowler, T. K., Jr., and Calzia, J. P., 1999, Kingston Range detachment fault, southeastern Death Valley region, California; relation to Tertiary deposits and reconstruction of initial dip, in Wright Lauren, A., and Troxel Bennie, W., eds., Cenozoic basins of the Death Valley region: Geological Society of America Special Paper 333, p. 245-257.

Frei, L.S., Magill, J.R., and Cox, A., 1984, Paleomagnetic results from the central Sierra Nevada: Constraints on reconstructions of the western United States: Tectonics, v. 3, p. 157-177.

Frei, L.S., 1986, Additional paleomagnetic results from the Sierra Nevada: Further constriants on Basin and Range extension and northward displacement in the western United States: Geological Society of America Bulletin, v. 97, p. 840-849.

Gans, P.B., and Miller, E.L., 1983, Style of mid-Tertiary extension in east-central Nevada., p. 107-160: Utah Geology and Mineral Survey Special Studies 59, p. 107-160.

Gans, P.B., Miller, E.L., McCarthy, J., and Ouldcott, M.L., 1985, Tertiary extensional faulting and evolving ductile-brittle transition zones in the northern Snake Range and vicinity; new insights from seismic data: Geology, v. 13, p. 189-193.

Gans, P.B., 1997, Large-magnitude Oligo-Miocene extension in southern Sonora: Implications for the tectonic evolution of northwest Mexico: Tectonics, v. 16, p. 388-408.

Glazner, A. F., Bartley, J. M., and Walker, J. D., 1989, Magnitude and significance of Miocene crustal extension in the central Mojave Desert, California; reply: Geology (Boulder), v. 17, no. 11, p. 1061-1062.

Glazner, A. F., Walker, J. D., Bartley, J. M., and Fletcher, J. M., 2002, Cenozoic evolution of the Mojave Block of Southern California, in Glazner Allen, F., Walker, J. D., and Bartley John, M., eds., Geologic evolution of the Mojave Desert and southwestern Basin and Range: Geological Society of America Memoir 195, p. 19-41

Goodman, E.D., and Malin, P.E., 1992, Evolution of the southern San Joaquin Basin and mid-Tertiary “transitional” tectonics, central California: Tectonics, v. 11, p. 478-498.

Graham, S. A., Stanley, R. G., Bent, J. V., and Carter, J.R., 1989, Oligocene and Miocene paleogeography of central California and displacement along the San Andreas fault: Geological Society of America Bulletin, v. 101, p. 711-730.

Guth, P. L., 1989, Day 4. Tertiary extension in the Sheep Range Area, Northwestern Clark County, Nevada, in Wernicke, B. P., Snow, J.K., Axen, G.J., Burchfiel, B.C., Hodges, K.V., Walker, J.D., and Guth, P.L., ed., Extensional tectonics in the Basin and Range Province between the Southern Sierra Nevada and the Colorado Plateau: Field Trip Guidebook T138, 28th International Geological Congress, American Geophysical Union, 80 p., p. 33-39.

Hamilton, W.B., 1987, Mesozoic geology and tectonics of the Big Maria Mountains region, southeastern California, in Dickinson William, R., and Klute Margaret, A., eds., Mesozoic rocks of southern Arizona and adjacent areas., Volume 18: Arizona Geological Society Digest: Tucson, AZ, United States, Arizona Geological Society, p. 33-47.

Hardyman, R.F., Ekren, E.B., and Proffett, J., 1984, Tertiary Tectonics of West-central Nevada - Yerington to Gabbs Valley, Western Geological Excursions, Guidebook, Volume 4, Mackay School of Mines, Department of Geological Sciences, p. 160-231.

Henry, C. D., 1989, Late Cenozoic Basin and Range structure in western Mexico adjacent to the gulf of California: Geological Society of America Bulletin, v. 101, p. 1147–1156.

Henry, C. D., and Aranda-Gomez, J. J., 2000, Plate interactions control Middle–Late Miocene, proto-Gulf and Basin and Range extension in the southern Basin and Range province: Tectonophysics, v. 318, p. 1–26.

Hintze, L. F., 1973, Geologic Road Logs of Western Utah and Eastern Nevada: Brigham Young University Research Studies, Geology Series, v. 20, p. art 2, no.7, 66.

Hoisch, T. D., and Simpson, C., 1993, Rise and tilt of metamorphic rocks in the lower plate of a detachment fault in the Funeral Mountains, Death Valley, California: Journal of Geophysical Research, v. 98, no. 4, p. 6805-6827.

Holm, D. K., and Dokka, R. K., 1991, Major late Miocene cooling of the middle crust associated with extensional orogenesis in the Funeral Mountains, California: Geophysical Research Letters, v. 18, no. 9, p. 1775-1778.

Holm, D. K., Snow, J. K., and Lux, D. R., 1992, Thermal and barometric constraints on the intrusive and unroofing history of the Black Mountains; implications for timing, initial dip, and kinematics of detachment faulting in the Death Valley region, California: Tectonics, v. 11, no. 3, p. 507-522.

Holm, D. K., Geissman, J. W., and Wernicke, B., 1993, Tilt and rotation of the footwall of a major normal fault system; paleomagnetism of the Black Mountains, Death Valley extended terrane, California: Geological Society of America Bulletin, v. 105, no. 10, p. 1373-1387.

Holm, D. K., and Dokka, R. K., 1993, Interpretation and tectonic implications of cooling histories; an example from the Black Mountains, Death Valley extended terrane, California: Earth and Planetary Science Letters, v. 116, no. 1-4, p. 63-80.

Holt W.E., Chamot-Rooke N, Le Pichon X , et al., 2000Velocity field in Asia inferred from Quaternary fault slip rates and Global Positioning System observations  Journal of Geophysical Research v. 105, p. 9185-19209

Hope, R.A., 1966, Geology and structural setting of the eastern Transverse Ranges, southern California [Ph.D. thesis]: Los Angeles, University of California.

Hornafius, J. S., Luyendyk, B.P., Terres,R.R., Kamerling,M.J., 1986, Timing and extent of Neogene tectonic rotation in the western Transverse Ranges, California: Geological Society of America Bulletin, v. 97, p. 1476-1487.

Houseman, G., England, P., 1986. Finite strain calculations of continental deformation.1. method and general results for convergent zones Journal of Geophysical Research, v. 91, p. 3651-3663.

Howard, K. A., and Miller, D. M., 1992, Late Cenozoic faulting at the boundary between the Mojave and Sonoran blocks; Bristol Lake area, California, in Richard Stephen, M., ed., Deformation associated with the Neogene, eastern California shear zone, southeastern California and southwestern Arizona; proceedings.: San Bernardino County Museum Association Special Publication: Redlands, CA, United States, San Bernardino County Museum Association, p. 37-47.

Hudson, D. M., Oriel, W.M., 1979, Geologic map of the Buckskin Range, Nevada, scale 1:1 8,000.

Hudson, M. R., Sawyer, D. A., and Warren, R. G., 1994, Paleomagnetism and rotation constraints for the middle Miocene southwestern Nevada volcanic field: Tectonics, v. 13, no. 2, p. 258-277.

Humphreys, E.D., Clayton, R.W., and Hager, B.H., 1984, A tomographic image of mantle structure beneath southern California: Geophysical Research Letters, v. 11, no. 7, p. 625-327.

Humphreys, E. D., 1995, Post-Laramide removal of the Farallon slab, western United States: Geology, v. 23, p. 987–990.

Ingersoll, R. V., Devaney, K.A., Geslin, J.K., Cavazza, W., Diamond, D.S., Heins, W.A., Jagiello, K.J., Marsaglia, K.M., Paylor, E.D., II, and Short, P.F., 1996, The Mud Hills, Mojave Desert, California: structure, stratigraphy, and sedimentology of a rapidly extended terrane: Geological Society of America Special Paper 303, p. 61-84.

Ingersoll, R. V., 2001, Structural and stratigraphic evolution of the Rio Grande Rift, northern New Mexico and southern Colorado: International Geology Review, v. 43, no. 10, p. 867-891.

Jackson, M., 1991, Paleoseismology of Utah, Volume 3: The number and timing of Holocene paleoseismic events on the Nephi and Levan segments, Wasatch fault zone, Utah: Utah Geological Survey Special Study 78, 23 p.

John, B. E. and Foster, D.A., 1993, Structural and thermal constraints on the initiation angle of detachment faulting in the southern Basin and Range: The Chemehuevi Mountains case study: Geological Society of America Bulletin, v. 105, p. 1091-1108.

Lavier L.L. and Buck W.R., 2002, Half graben versus large-offset low-angle normal fault: Importance of keeping cool during normal faulting: Journal of Geophysical Research v. 107 2122, doi:10.1029/2001JB000513.

Lee, J., 1995, Rapid uplift and rotation of mylonitic rocks from beneath a detachment fault: Insights from potasium feldspar 40Ar/ 39Ar thermochronology, northern Snake Range, Nevada: Tectonics, v. 3, p. 54-77.

Lee, J., Miller, M.M., Crippen, R., Hacker, B. and Ledesma Vazquez, J., 1996, Middle Miocene extension in the Gulf Extensional Province, Baja California: Evidence from the southern Sierra Juarez: Geological Society of America Bulletin, v. 108, p. 505-525.

Lewis, C. J., Wernicke, B.P., Selverstone, J., and Bartley, J.M., 1999, Deep burial of the footwall of the northern Snake Range decollement, Nevada: Geological Society of America Bulletin, v. 111, p. 39-51.

Long, K. B., Baldwin, S.L., and Gehrels, G.E., 1995, Tectonothermal evolution of the Pinaleno-Jackson Mountain core complex, southeast Arizona: Geological Society of America Bulletin, v. 107, p. 1231-1240.

Lund, K., Beard, S.L., Perry, W.J., 1993, Relation between extensional geometry of the northern Grant Range and oil occurrences in Railroad Valley, east-central Nevada: AAPG Bulletin, v. 77, p. 945-962.

Luyendyk, B. P., 1991, A model for Neogene crustal rotations, transtension, and transpression in southern California: Geological Society of America Bulletin, v. 103, p. 1528-1536.

Machette, M.N., Personius, S.F., and Nelson, A.R., 1992, Paleoseismology of the Wasatch fault zone; a summary of recent investigations, interpretations, and conclusions, in Gori, Pl., and Hays, W.W.. Assesment of Regional Earthquake Hazards and Risk Along the Wasatch Front, Utah, Professional Paper 1500-A p A1-A71, US Geological Survey, Reston, VA.

Martin, M.W., Glazner, A.F., Walker, J.D., and Schermer, E.R., 1993, Evidence for right-lateral transfer faulting accommodating en echelon Miocene extension, Mojave Desert, California: Geology, v. 21, p. 355–358.

Matthews, V., III, 1976, Correlation of Pinnacles and Neenach volcanic formations and there bearing on the San Andreas problem: AAPG Bulletin, v. 51, p. 2128-2141.

McClusky, S.S., Bjornstad, S., Hager, B., King, R., Meade, B., Miller, M., Monastero, F., and Souter, B., 2001, Present day kinematics of the Eastern California Shear Zone from a geodetically constrained block model: Geophysical Research Letters, v. 28, p. 3369-3372.

McQuarrie, N. , Stock J.M., Verdel, C., Wernicke, B.P., 2003, Cenozoic evolution of Neotethys and implications for the causes of plate motions. Geophysical Research Letters, v. 30, p. 2036.

McWilliams, M. O., and Li, Y., 1985, Oroclinal folding of the southern Sierra Nevada batholith: Science, v. 230, p. 172-175.

Miller, D.M., and Yount, J.C., 2002, Late Cenozoic tectonic evolution of the north-central Mojave Desert inferred from fault history and physiographic evolution of the Fort Irwin area, in Glazner Allen, F., Walker, J.D., and Bartley John, M., eds., Geologic evolution of the Mojave Desert and southwestern Basin and Range: Geological Society of America Memoir 195, p. 173-198.

Miller, E.L., Gans, P.B., and Garing., J., 1983, The Snake Range decollement: An exhumed mid-Tertiary ductile-brittle transition: Tectonics, v. 2, p. 239-263.

Miller, E. L., Dumitru, T. A., Brown, R. W., and Gans, P. B., 1999, Rapid Miocene slip on the Snake Range-Deep Creek Range fault system, east-central Nevada: Geological Society of America Bulletin, v. 111, no. 6, p. 886-905.

Miller, F. K., and Morton, D. M., 1980, Potassium-argon geochronology of the eastern Transverse Ranges and southern Mojave Desert, southern California, U. S. Geological Survey Professional Paper: Reston, VA, United States, U. S. Geological Survey, 30 p.

Miller, M., Johnson, D., Dixon, T., and Dokka, R.K., 2001, Refined kinematics of the eastern California shear zone from GPS observations, 1993 – 1998: Journal of Geophysical Research, v. 106, p. 2245-2263.

Namson, J. S., Davis, T. L., 1990, Late Cenozoic fold and thrust belt of the southern Coast Ranges and Santa Maria Basin, California, AAPG Bulletin, v.74, p.467-492.

Namson, J. S., Davis, T. L., 1988a, Structural transect of the western Transverse Ranges, California; Implications for lithospheric kinematics and seismic risk evaluation; Geology, v.16, p.675-679.

Namson, J. S., Davis, T. L., 1988b, Seismically active fold-thrust belt in the San Joaquin Valley, central California, Geology, v.16, p.675-679.

Niemi, N.A., 2002, Extensional Tectonics in the Basin and Range Province and the Geology of the Grapevine Mountains,Death Valley Region,California and Nevada [Ph.D. thesis], California Institute of Technology.

Niemi, N. A., Wernicke, B. P., Friedrich, A. M., Simons, M., Bennett, R. A., and Davis, J. L., 2004, BARGEN continuous GPS data across the eastern Basin and Range province, and implications for fault system dynamics: Geophysical Journal International, v. 159, p. 842-862.

Niemi, N.A., Wernicke, B.P., Brady, R.J., Saleeby, J.B., and Dunne, G.C., 2001, Distribution and provenance of the middle Miocene Eagle Mountain Formation, and implications for regional kinematic analysis of the Basin and Range province: Geological Society of America Bulletin, v. 113, p. 419-442.

Nourse, J.A., Anderson, T.H., and Silver, L.T., 1994, Tertiary metamorphic core complexes in Sonora, northwestern Mexico: Tectonics, v. 13, p. 1161-1182.

Oskin, M., and Iriondo, A., 2004, Large magnitude transient strain accumulation on the Blackwater fault, Eastern California shear zone: Geology, v. 32, p. 313-316.

Oskin, M., Stock, J., Martin-Barajas, A, 2001, Rapid localization of Pacific-North America plate motion in the Gulf of California: Geology, no. 29, p. 459-462.

Page, B.M., Thompson, G.A., and Coleman, R.G., 1998, Late Cenozoic tectonics of the central and southern ranges of California: Geological Society of America Bulletin, v. 110, p. 846-876.

Plescia, J B, Calderone, G. J, 1986, Paleomagnetic constraints on the timing and extent of rotation of the Tehachapi Mountains, California: Abstracts with Programs - Geological Society of America, v.18, p.171.

Powell, R. E., 1981, Geology of the crystalline basement complex, eastern Transverse Ranges, southern California: Constraints on regional tectonic interpretation: California Institute of Technology,, 441 p.

Reheis, M. C., 1993, Neogene tectonism from the southwestern Nevada volcanic field to the White Mountains, California; Part II, Late Cenozoic history of the southern Fish Lake Valley fault zone, Nevada and California, in Lahren, M. M., Trexle, J.H., Jr., and Spinosa, C., eds., Crustal evolution of the Great Basin and the Sierra Nevada.: Reno, NV, United States, University of Nevada, p. 370-382.

Reheis, M. C., and Sawyer, T. L., 1997, Late Cenozoic history and slip rates of the Fish Lake Valley, Emigrant Peak, and Deep Springs fault zones, Nevada and California: Geological Society of America Bulletin, v. 109, no. 3, p. 280-299.

Reynolds, S. J., 1985, Geology of the South Mountains, central Arizona: Arizona Bureau of Geology and Mineral Technology Bulletin, v. 195, p. 61 p.

Richard, S. M., Fryxell, J.E., and Sutter, J.F., 1990, Tertiary structure and thermal history of the Harquahala and Buckskin Mountains, west central Arizona: Implications for denudation by a major detachment fault system: Journal of Geophysical Research, v. 95, p. 19973-19987.

Richard, S. M., and Dokka, R. K., 1992, Geology of the Packard Well fault zone, southeastern California, in Richard Stephen, M., ed., Deformation associated with the Neogene, eastern California shear zone, southeastern California and southwestern Arizona; proceedings: San Bernardino County Museum Association Special Publication: Redlands, CA, United States, San Bernardino County Museum Association, p. 71-74.

Richard, S. M., Sherrod, D. R., and Tosdal, R. M., 1992, Cibola Pass Fault, southwestern Arizona, in Richard Stephen, M., ed., Deformation associated with the Neogene, eastern California shear zone, southeastern California and southwestern Arizona; proceedings: San Bernardino County Museum Association Special Publication: Redlands, CA, United States, San Bernardino County Museum Association, p. 66-70.

Richard, S. M., 1993, Palinspastic reconstruction of southeastern California and southwestern Arizona for the Middle Miocene: Tectonics, v. 12, p. 830-854.

Ron, H., and Nur, A., 1996, Vertical axis rotation in the Mojave; evidence from the Independence dike swarm: Geology, v. 24, no. 11, p. 973-976.

Rotstein, Y., Combs, J., Biehler, S., 1976, Gravity investigation in the southern Mojave Desert. California: Geological Society of America Bulletin, v. 87, p. 981-993.

Russell, L. R., and Snelson, S., 1994, Structure and tectonics of the Albuquerque Basin segment of the Rio Grande Rift; insights from reflection seismic data, in Keller, G. R., and Cather Steven, M., eds., Basins of the Rio Grande Rift; structure, stratigraphy, and tectonic setting.: Special Paper - Geological Society of America: Boulder, CO, United States, Geological Society of America (GSA), p. 83-112.

Sauber, J., Thatcher, W., Solomon, S., and Lisowski, M., 1994, Geodetic slip rate for the eastern California shear zone and the recurrence time of Mojave desert earthquakes: Nature, v. 367, p. 264-266.

Savage, J.C., Lisowski, M., and Prescott, W., 1990, An apparent shear zone trending north-northwest across the Mojave Desert into Owens Valley, eastern California: Geophysical Research Letters, v. 17, p. 2113-2116.

Schermer, E. R., Luyendyk, B. P., and Cisowski, S., 1996, Late Cenozoic structure and tectonics of the northern Mojave Desert: Tectonics, v. 15, no. 5, p. 905-932.

Scott, R. J., Foster, D.A., Lister, G.S., 1998, Tectonic implications of rapid cooling of lower plate rocks from the Buckskin-Rawhide metamorphic core complex,west-central Arizona: Geological Society of America Bulletin, v. 110, p. 588-614.

Sieh, K., and Jahns, R. H., 1984, Holocene activity of the San Andreas Fault at Wallace Creek, California: Geological Society of America Bulletin, v. 95, p. 883-896.

Smith, D. L., Gans, P.B., Miller, E.L., 1991, Palinspastic restoration of Cenozoic extension in the central and eastern Basin and Range Province at latitude 39-40 degrees N, in Raines, G. L., Lisle, R.E., Schafer, R.W., Wilkinson, W.H., ed., Geology and ore deposits of the Great Basin; symposium proceedings.: Reno, NV, Geological Society of Nevada, p. 75-86.

Smith, D. L., 1992, History and kinematics of Cenozoic extension in the northern Toiyabe Range, Lander County, Nevada: Geological Society of America Bulletin, v. 104, p. 789-801.

Smith, R.B., and Bruhn, R.L., 1984, Intraplate extensional tectonics of the western U.S. Cordillera-Inferences on structural style from seismic-reflection data, regional tectonics and thermal-mechanical models of brittle ductile deformation: Journal of Geophysical research, v. 89, p. 5733-5762.

Snow, J. K., and Wernicke, B. P., 1989, Uniqueness of geological correlations; an example from the Death Valley extended terrain: Geological Society of America Bulletin, v. 101, no. 11, p. 1351-1362.

Snow, J. K., 1992, Large-magnitude Permian shortening and continental margin tectonics in the southern Cordillera: Geological Society of America Bulletin, v. 104, no. 1, p. 80-105.

Snow, J. K., and Prave, A. R., 1994, Covariance of structural and stratigraphic trends; evidence for anticlockwise rotation within the Walker Lane Belt, Death Valley region, California and Nevada: Tectonics, v. 13, no. 3, p. 712-724.

Snow, J. K., and Lux, D. R., 1999, Tectono-sequence stratigraphy of Tertiary rocks in the Cottonwood Mountains and northern Death Valley area, California and Nevada, in Wright Lauren, A., and Troxel Bennie, W., eds., Cenozoic basins of the Death Valley region.: Geological Society of America Special Paper 333, p. 17-64.

Snow, J. K., and Wernicke, B.P, 2000, Cenozoic tectonism in the central Basin and Range: Magnitude, rate and distribution of upper crustal strain: American Journal of Science, v. 300, p. 659-719.

Spencer, J. E., and Reynolds, S. J., 1989, Middle Tertiary tectonics of Arizona and adjacent areas, in Jenney, J. P., and Reynolds Stephen, J., eds., Geologic evolution of Arizona.: Arizona Geological Society Digest: Tucson, AZ, United States, Arizona Geological Society, p. 539-574.

Spencer, J. E., and Reynolds, S. J., 1991, Tectonics of mid-Tertiary extension along a transect through west central Arizona: Tectonics, v. 10, no. 6, p. 1024-1221.

Spencer, J. E., Richard, S. M., Reynolds, S. J., Miller, R. J., Shafiqullah, M., Gilbert, W. G., and Grubensky, M. J., 1995, Spatial and temporal relationships between mid-Tertiary magnetism and extension in southwestern Arizona: Journal of Geophysical Research, B, Solid Earth and Planets, v. 100, no. 6, p. 10,321-10,351.

Stock, J.M., and Hodges, K.V., 1989, Pre-Pliocene extension around the Gulf of California and the transfer of Baja California to the Pacific Plate: Tectonics v.8, p. 99-115

Stockli, D. F., 1999, Regional timing and spatial distribution of Miocene extension in the northern Basin and Range Province [Ph.D. thesis]: Stanford University, 239 p.

Stockli, D. F., Linn, J.K., Walker, J.D., Dumitru, T.A., 2001, Miocene unroofing of the Canyon Range during extension along the Sevier Desert Detachment, west-central Utah: Tectonics, v. 20, p. 289-307.

Stockli, D. F., Surpless, B.E., Dumitru, T.A., and Farley, K.A., 2002, Thermochronological constraints on the timing and magnitude of Miocene and Pliocene extension in the central Wassuk Range, western Nevada: Tectonics, v. 21, no. 4, p. 10.1029/2001TC001295.

Stone, P., and Pelka, G.J., 1989, Geologic Map of the Palen-McCoy Wilderness Study Area and vicinity, Riverside County, California, Geological Survey Miscellaneous Field Investigations Map MF-2070.

Surpless, B., 1999, Tectonic Evolution of the Sierra Nevada-Basin and Range transition zone: a study of crustal evolution in extensional provinces [Ph.D. thesis]: Stanford University, 186 p.

Taylor, W. J., Bartley, J.M., Lux, D.R., and Axen, G.J., 1989, Timing of Tertiary extension in the Railroad Valley-Pioche Transect, Nevada: Constraints from

40Ar/39Ar ages of volcanic rocks: Journal of Geophysical Research, v. 94, p. 7757-7774.

Tennyson, M.E., 1989, Pre-transform early Miocene extension in western California: Geology, v. 17. P. 792-796.

Walker, J. D., Bartley, J. M., and Glazner, A. F., 1990, Large-magnitude Miocene extension in the central Mojave Desert; implications for Paleozoic to Tertiary paleogeography and tectonics, Journal of Geophysical Research, v. 95, p. 557-569.

Walker, J.D., Fletcher, J.M., Fillmore, R.P., Martin, M.W., Taylor, W.J., Glazner, A.F., and Bartley, J.M., 1995, Connection between igneous activity and extension in the central Mojave metamorphic core complex, California: Journal of Geophysical Research, v. 100, p. 10477–10 494.

Wernicke, B.P., 1992, Cenozoic extensional tectonics of the U.S. Cordillera, in Burchfiel, B.C., Lipman, P.W., and Zoback, M.L., eds., The Cordilleran Orogen: Conterminous U.S. The Geology of North America, Volume G-3: Boulder, CO, Geological Society of America, p. 553-581.

Wernicke, B. P., Axen, G.J., Snow, J.K., 1988, Basin and Range extensional tectonics at the latitude of Las Vegas, Nevada: Geological Society of America Bulletin, v. 100, p. 1738-1757.

Wernicke, B. P., and Snow, J.K., 1998, Cenozoic tectonism in the central Basin and Range: Motion of the Sierran-Great Valley Block: International Geology Review, v. 40, p. 403-410.

Wills S, Anders M. H, and Christie-Blick, N., 2005, Pattern of Mesozoic thrust surfaces and tertiary normal faults in the Sevier Desert subsurface, west-central Utah: American Journal of Science, v. 305, p. 42-100.

# FIGURES

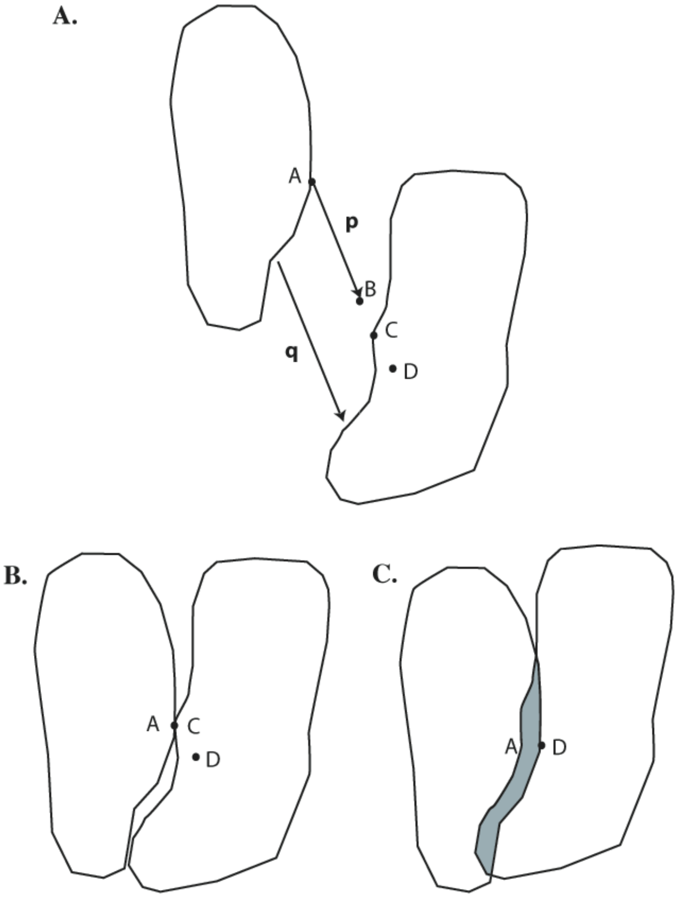

Figure 1.
Schematic diagram illustrating the method of using regional structural constraints to limit possible displacement paths in tectonic reconstructions. See text for discussion.

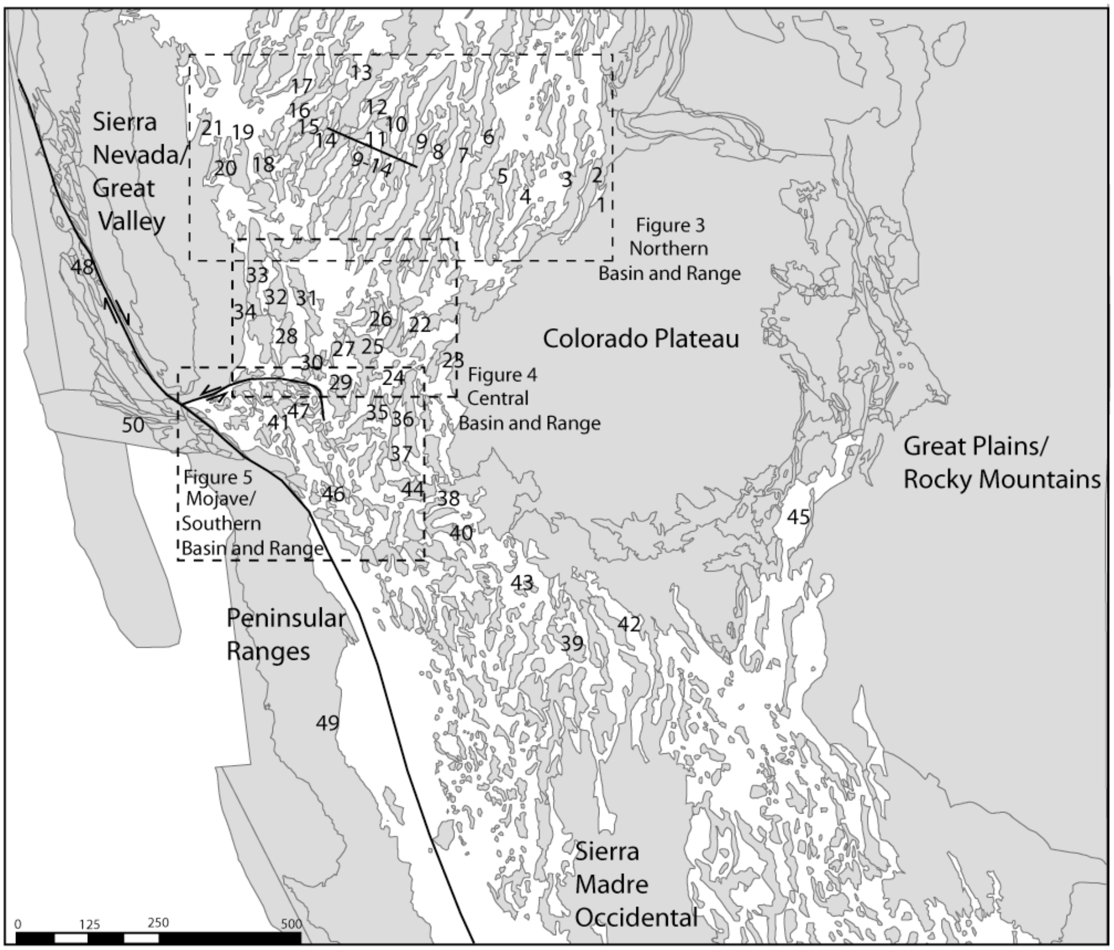

Figure 2.
Map of western North America showing the primary tectonic elements in the reconstruction. The shaded polygons represent the physiographic or geologic expression of mountain ranges, which in the Basin and Range are fault-bounded and separated by alluvial valleys. Dashed boxes are the locations of Figures 3 to 5. The numbers refer to specific mountain ranges identified in Tables 1-6.

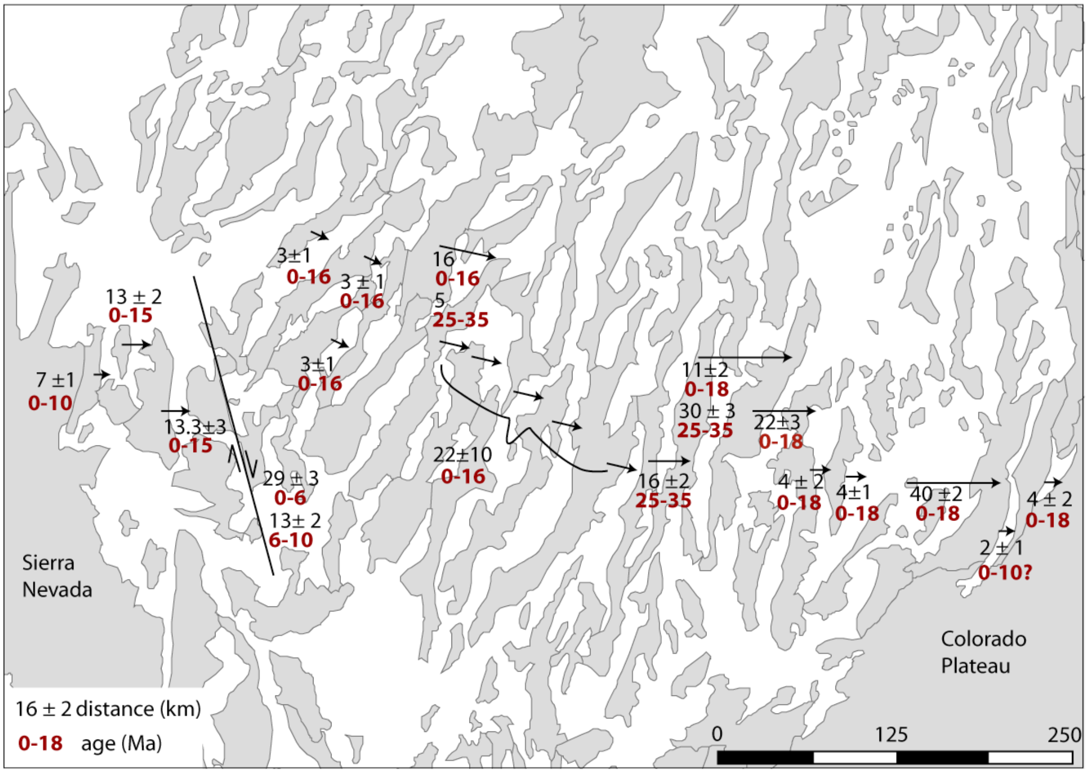

Figure 3.

Map of the northern Basin and Range showing the kinematic data incorporated into the model. Black numbers indicate horizontal displacement amount, red bold numbers indicates age range of motion. Arrows indicate approximate magnitude and direction of individual relative displacements between polygons. Data compiled from Allmendinger et al., 1986; Armstrong et al., 2004; Bartley and Wernicke, 1984; Coogan and DeCelles, 1996; DeCelles et al., 1995; Dilles and Gans, 1995; Faulds et al., 2003; Hardyman et al., 1984; Hintzi, 1973; Hudson and Oriel, 1979; Lee, 1999, Miller et al., 1999; Niemi, 2000; Niemi, et al., 2004; Smith, 1992; Smith et al., 1990; Smith and Bruhn, 1984; Stockli, 2000; 2001; Surpless, 1999.

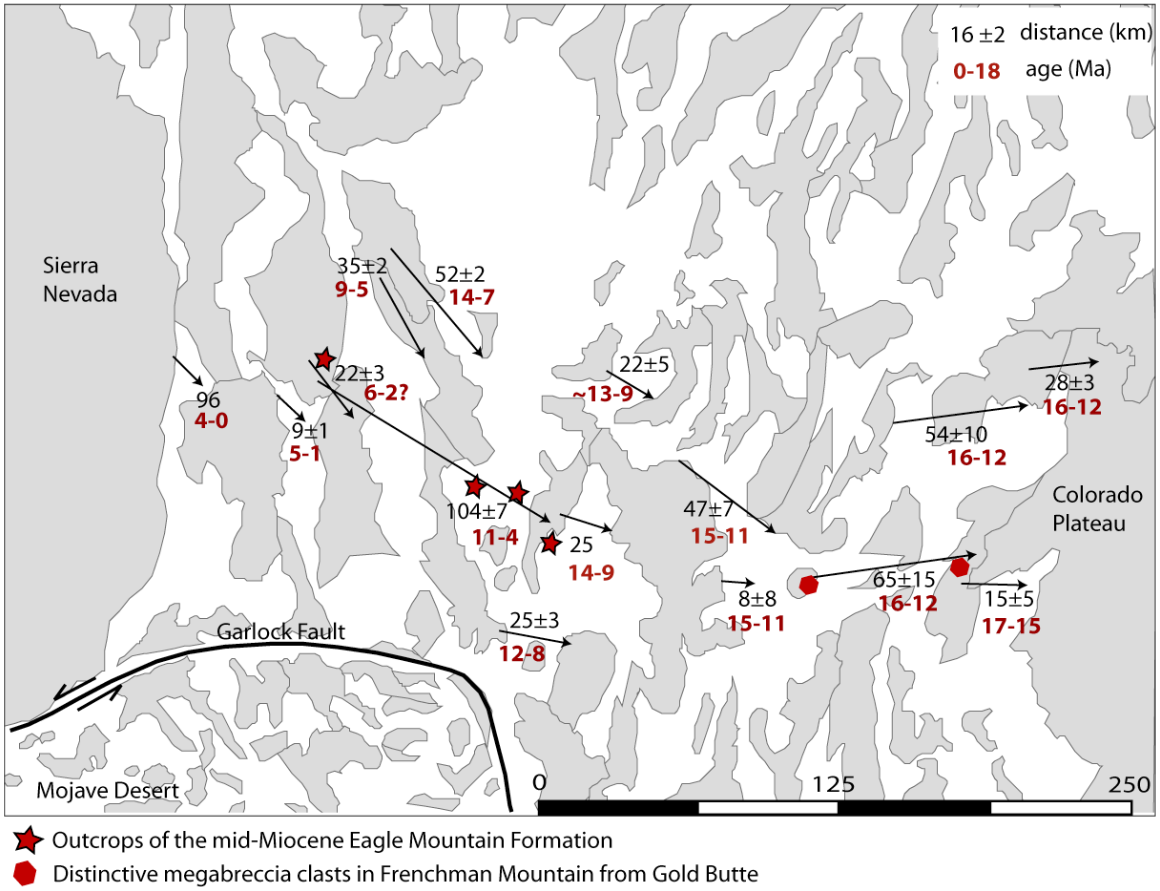

Figure 4.

Map of the central Basin and Range showing the kinematic data incorporated into the model. Motion of the Sierra Nevada with respect to the Colorado Plateau in this region is predominantly constrained by two distinctive sedimentary deposits (indicated as stars and hexagons) offset along extensive normal and strike-slip fault systems. Arrows indicate approximate magnitude and direction of individual relative displacements between polygons. Black numbers indicate horizontal displacement amount, bold red numbers indicates age range of displacement. Data from Axen et al., 1990; Brady et al., 2000; Burchfiel, 1968; Burchfiel et al., 1987; Cemen et al., 1985; Duebendorfer et al., 1998; Fitzgerald et al., 1991; Fowler and Calzia, 1999; Guth, 1989; Holm and Dokka, 1991;1993; Hoisch and Simpson, 1993; Niemi et al., 2001; Snow and Lux, 1999; Snow and Wernicke, 1989; 2000; Wernicke et al., 1988.

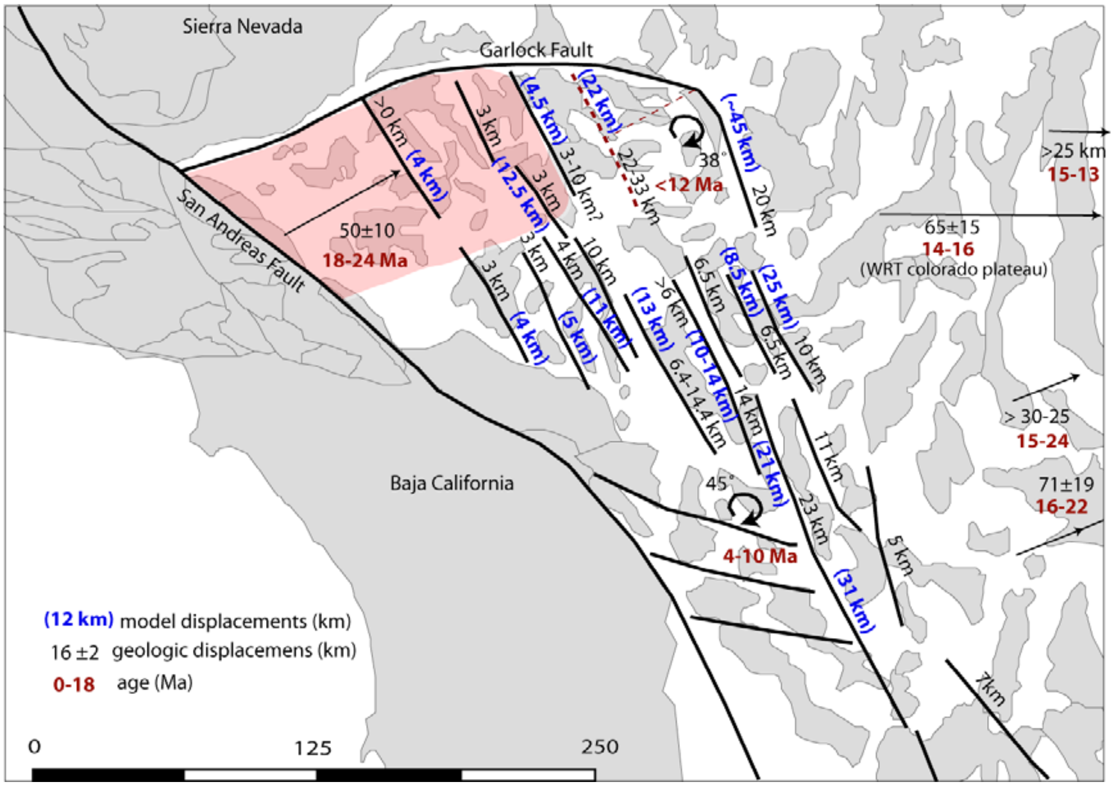

Figure 5.

Map of the Mojave and Southern Basin and Range region showing distribution of strike-slip faults (bold lines), vertical axis rotation data (curved arrows) and extensional offsets (straight arrows). For strike-slip faults, reported slip amounts (black numbers) are contrasted with model slip (bold blue numbers). For extension and rotation constraints, black numbers indicate horizontal displacement or amount or rotation, bold red numbers indicates age range of deformation. Data from Ballard, 1990; Bassett and Kupfer, 1964; Dokka, 1983; 1989; Foster et al., 1993; John and Foster, 1993; Hamilton, 1987; Howard and Miller, 1992; Miller, 1980; Miller and Morton, 1980; Powell, 1981; Richard et al., 1992; Richard, 1993; Richard and Dokka, 1992; Spencer and Reynolds, 1989; Spencer et al., 1995; Schermer et al., 1996; Walker et al, 1995.

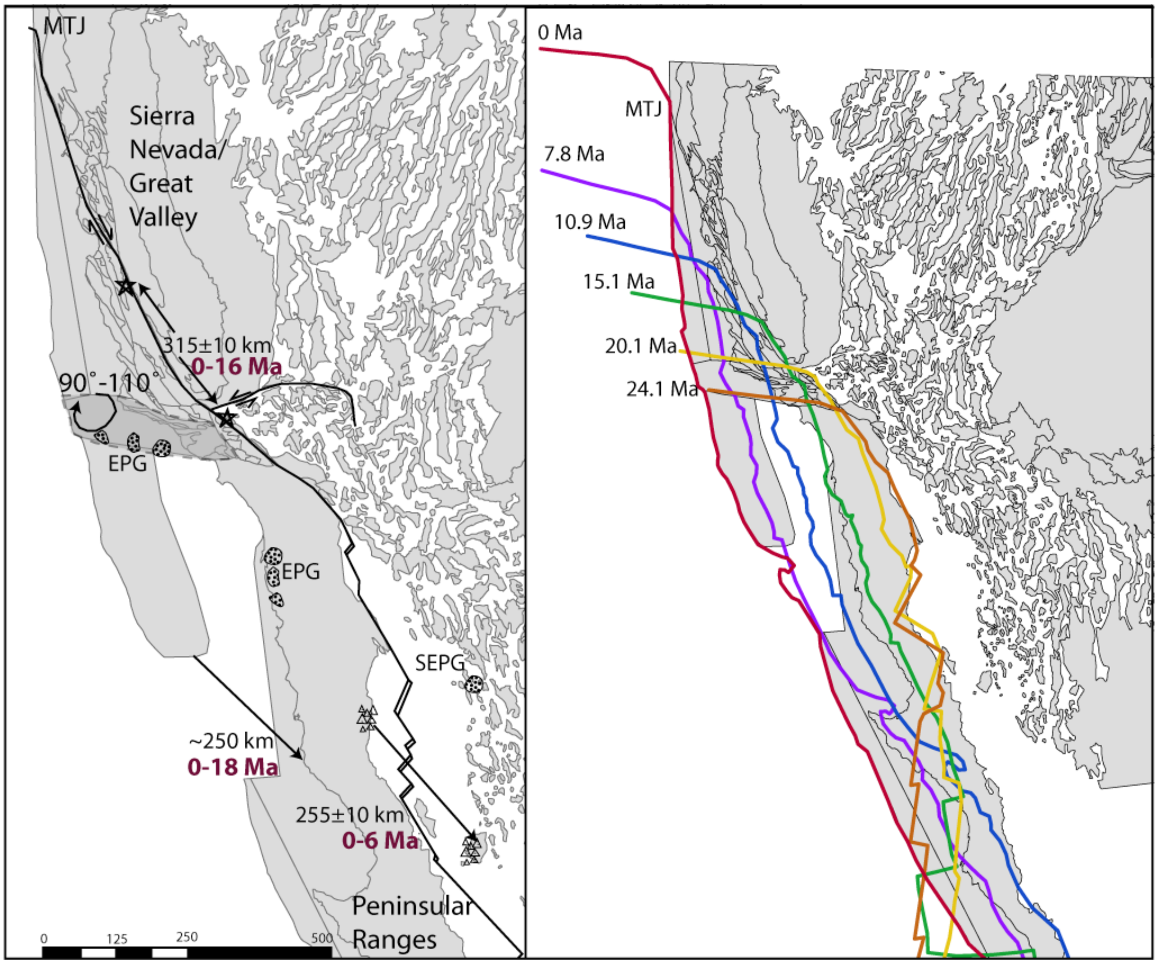

Figure 6.

A. First-order constraints for displacement along the San Andreas fault and associated displacements to the west. Arrows indicate approximate magnitude and direction of individual relative displacements between polygons. Black numbers indicate horizontal displacement amount, bold red numbers indicates age range of displacement. Stippled areas labeled EPG show distribution of Eocene Poway Group and equivalents. Stippled area labeled SEPG marks the location of the source area for the Eocene Poway Group Triangle pattern (Gulf of California) and stars (central California) show distribution of correlative volcanic units offset by the San Andreas/Gulf of California rift system. Data from Abbott and Smith, 1989; Bohannon and Geist, 1998; Crouch and Suppe, 1993; Dickinson and Wernicke, 1997; Dickinson, 1996; Graham et al., 1989; Hornafius et al., 1986; Luyendyk, 1991, Matthews, 1979; Oskin et al., 2001. B. Successive locations of the eastern edge of Pacific plate oceanic lithosphere relative to stable North America. The thick colored lines represent minimum extent of oceanic lithosphere at the times shown. (from Atwater and Stock, 1998). These positions constrain the maximum westward extent of continental North America through time.

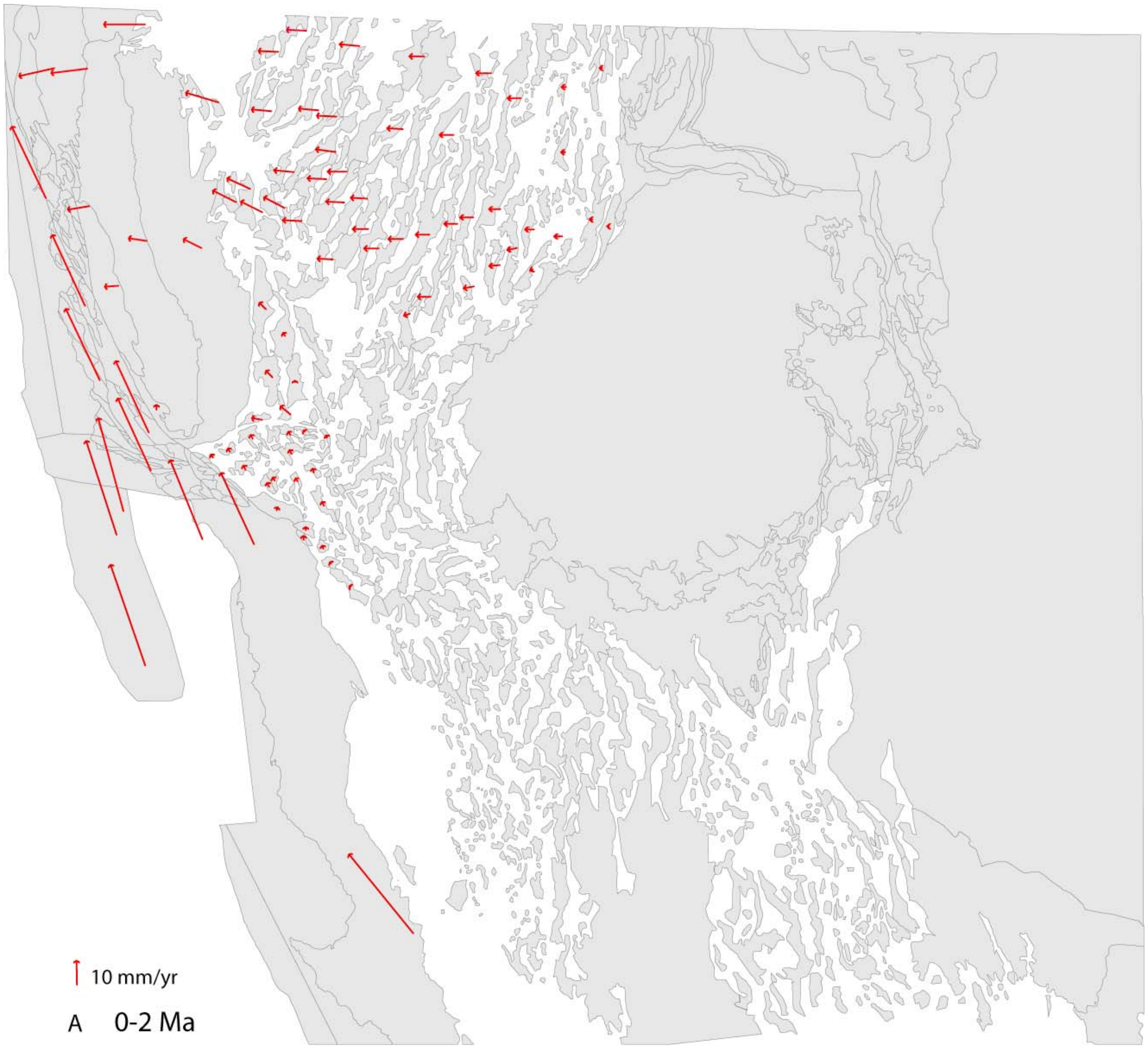
10 mm/yr
A
0-2 Ma

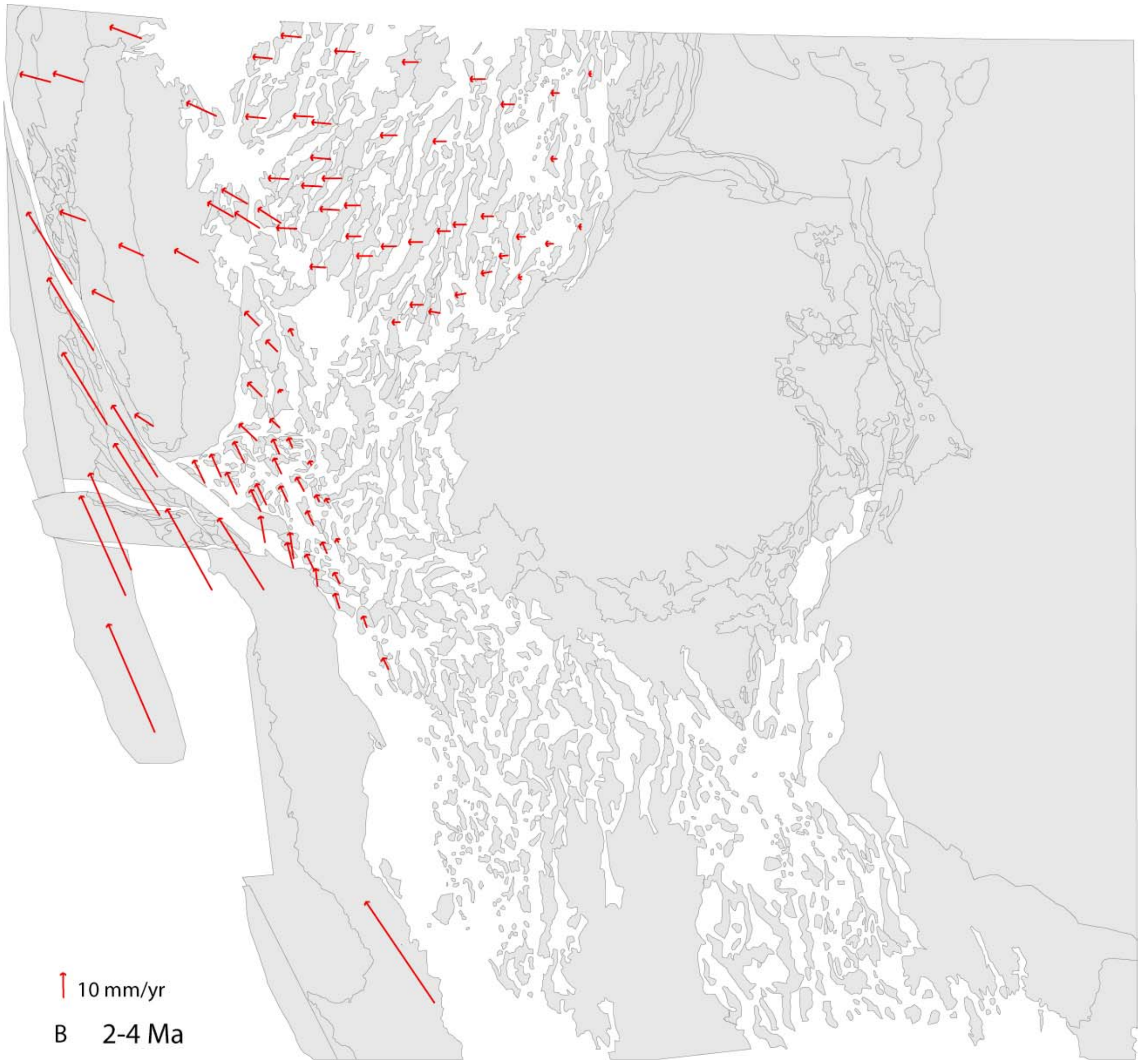
10 mm/yr
B
2-4 Ma

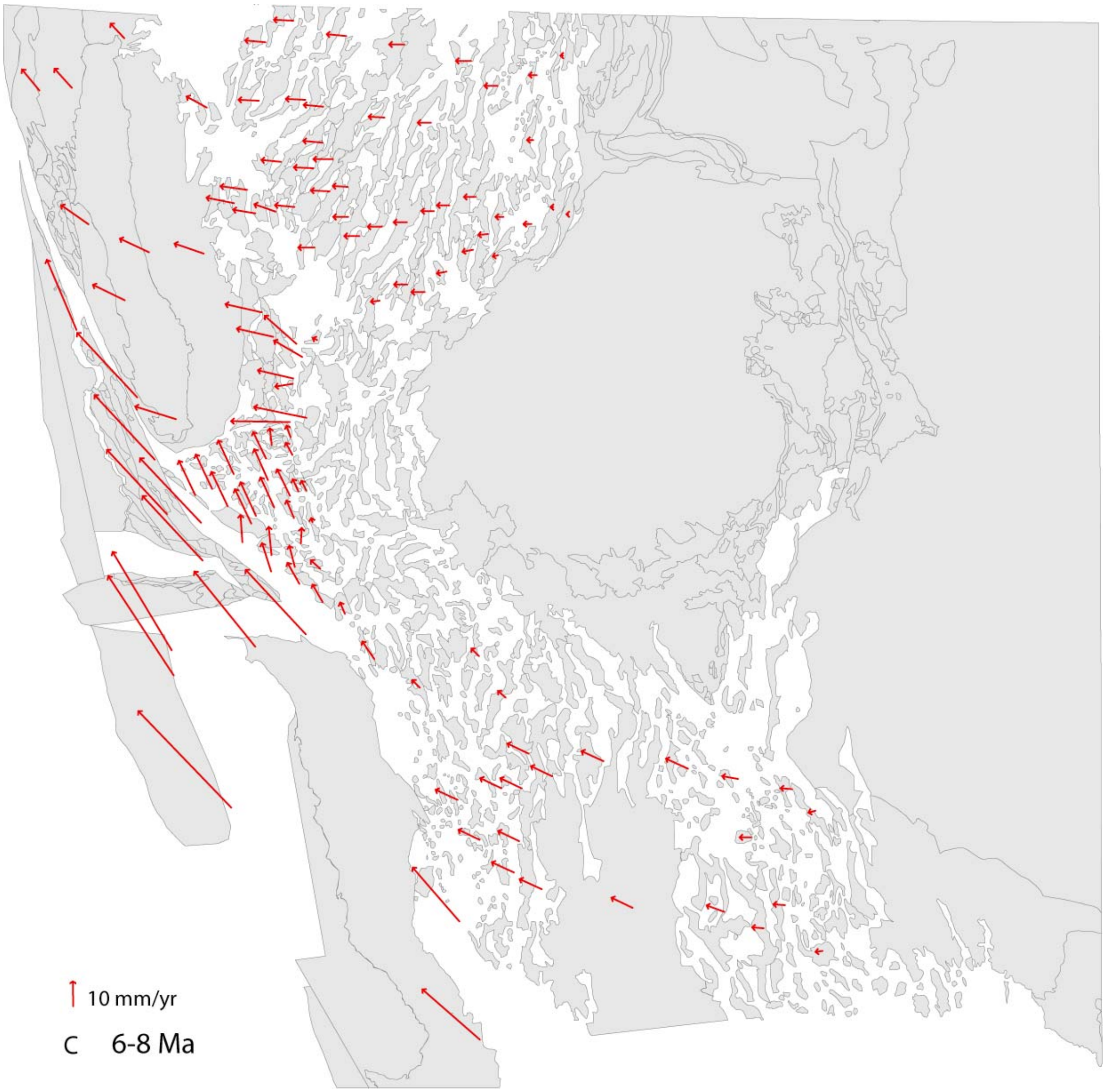
10 mm/yr
C
6-8 Ma

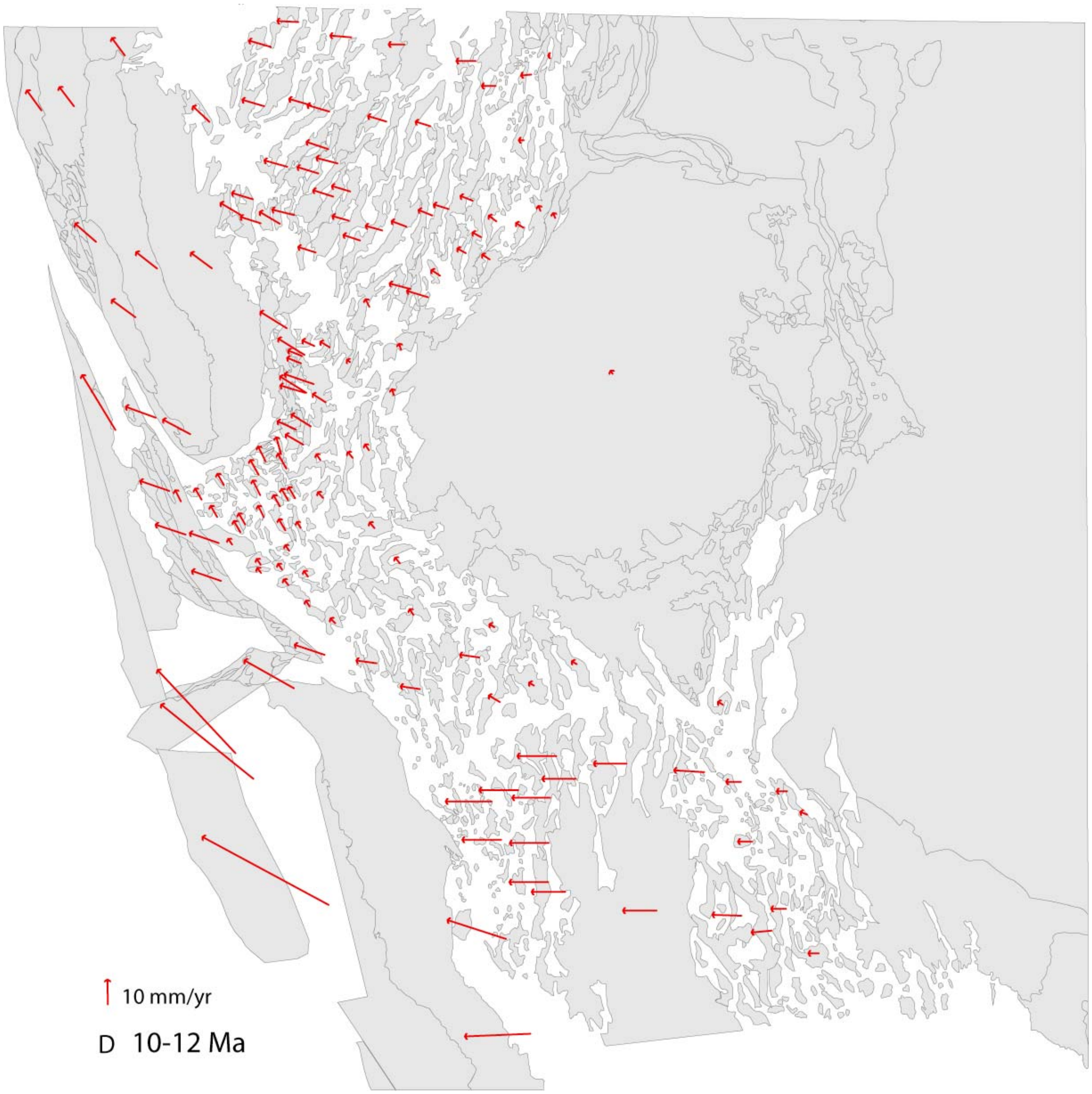
10 mm/yr
D 10-12 Ma

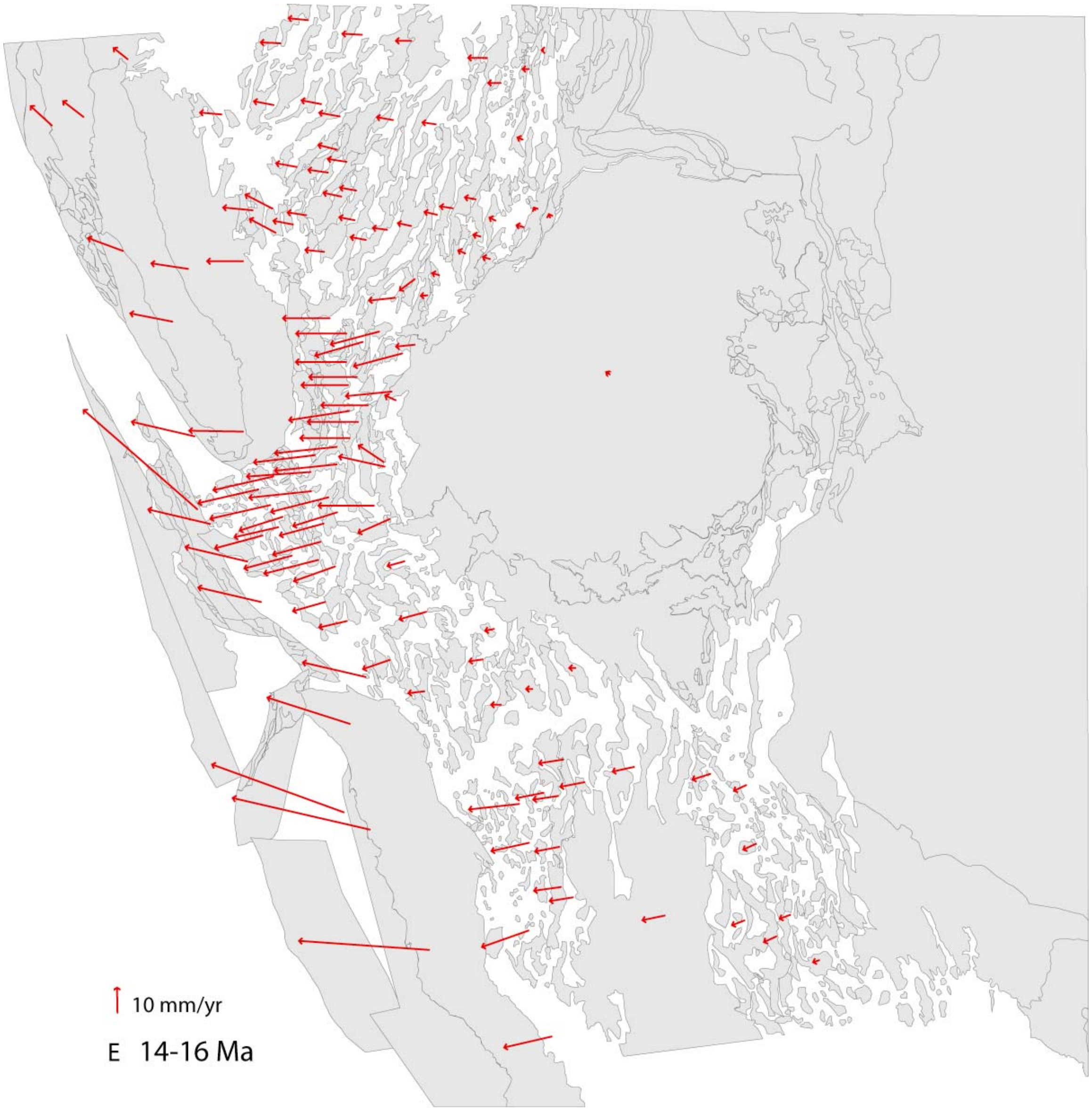

E 14-16 Ma

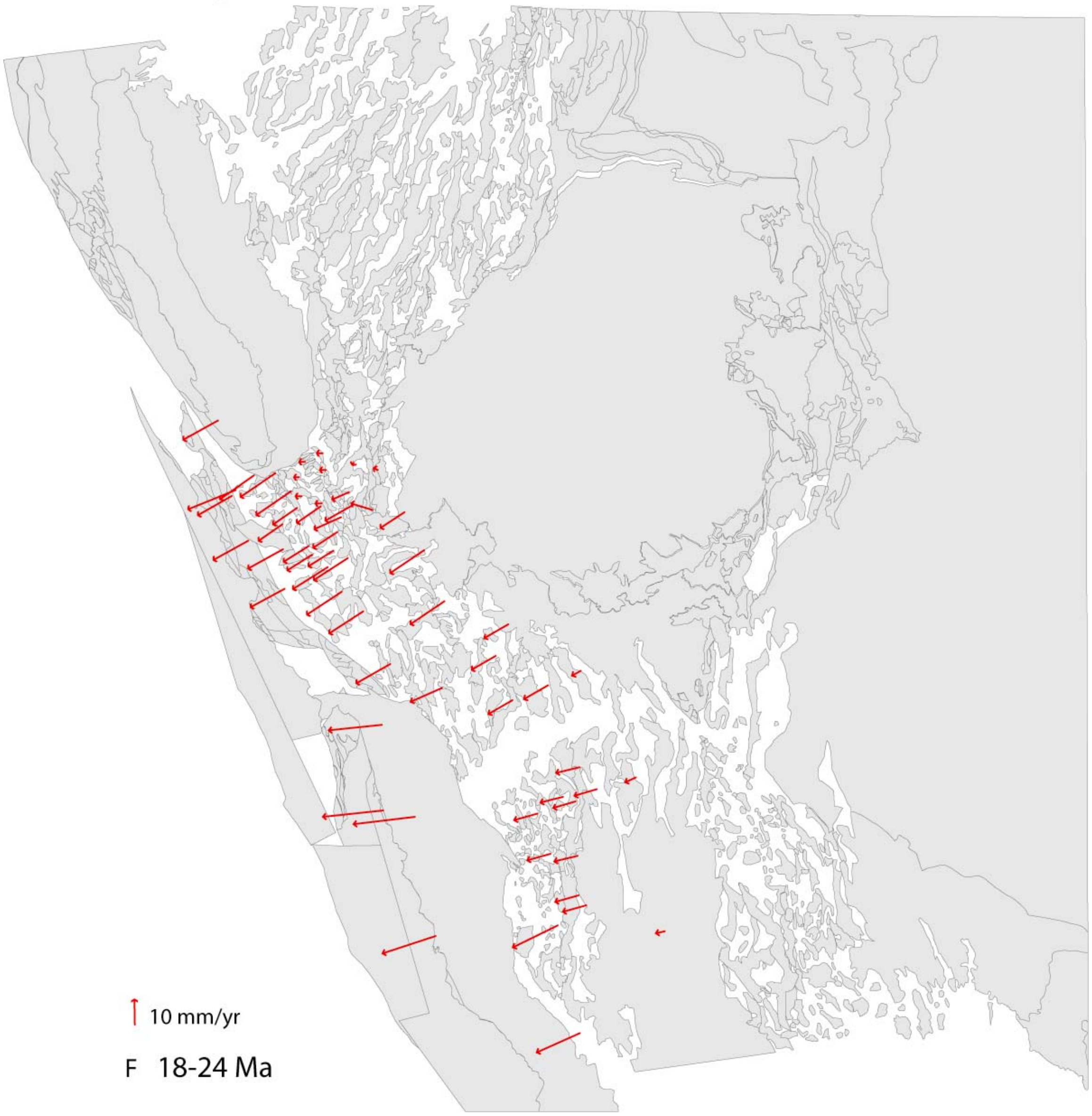

F 18-24 Ma

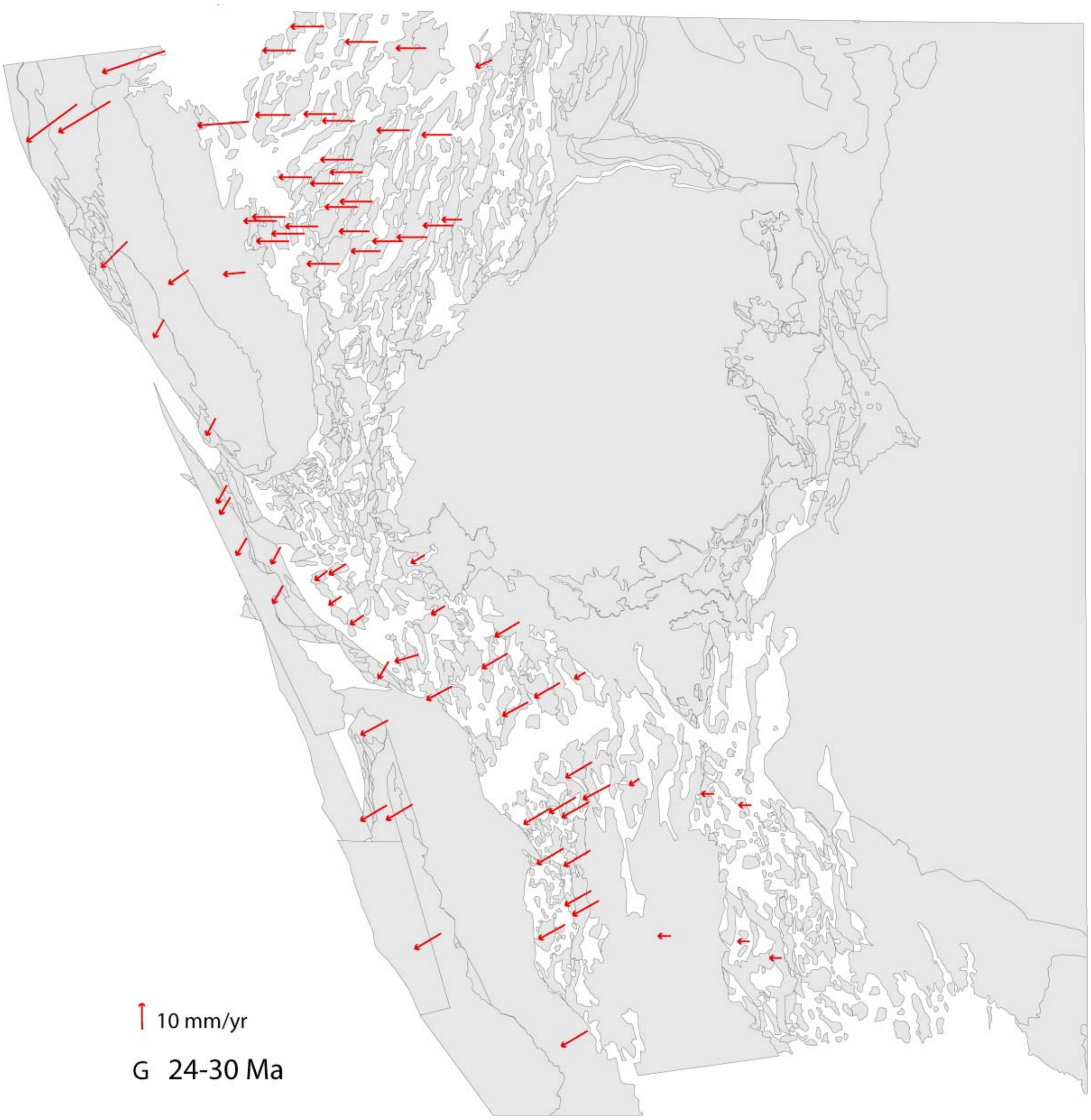

Figure 7. "Instantaneous" velocity fields based on 2 Myr averages from 0 to 18 Ma, and 6 Myr averages from 18 to 36 Ma. Arrows show displacement with respect to stable North America and were determined by connecting the centroids of specific ranges at one time with the centroid of the same range in a later time. Because the motion of individual ranges can be very slight at the eastern edge of the model, the line lengths representing each incremental offset were uniformly doubled. Map base is the palinspastic map from the youngest time in the 2 or 6 Myr interval.

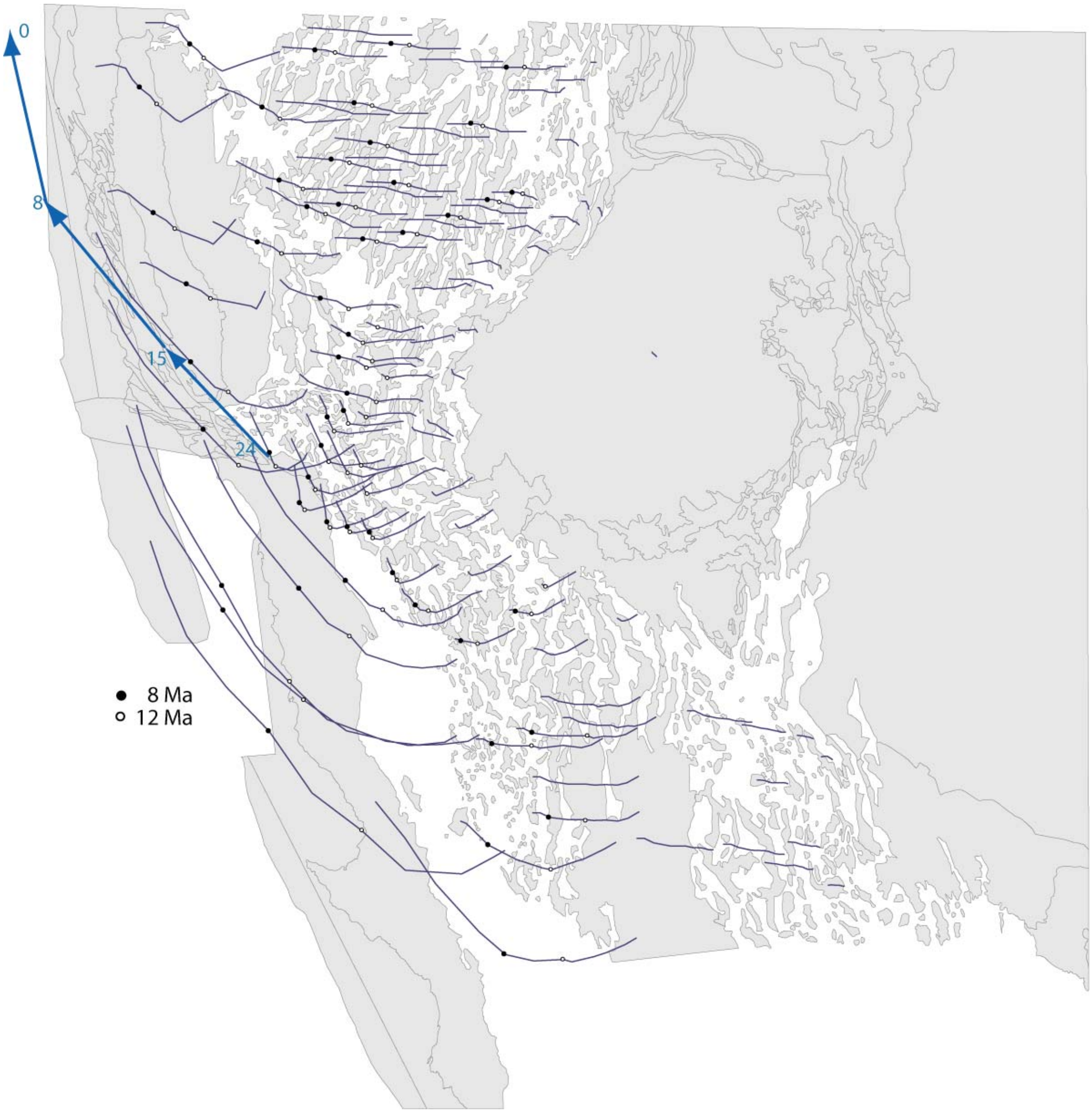

Figure 8. Map illustrating paths of various ranges from 0-36 Ma.. Solid black circles indicate the positions of the ranges at 8 Ma, and open circles represent the positions of the ranges at 12 Ma. The westernmost point on each line represents the current location of each range. The easternmost point on the path represents the location of the range at 36 Ma. The blue arrows represent the motion of the Mendicino triple junction, with its position shown at 24, 15, 8 and 0 Ma (Atwater and Stock, 1998).

| Northern Basin and Range latitude of 40° N | | | | | | | | |
|---|---|---|---|---|---|---|---|---|
| | | | | | | | | |
| Range/fault | Horizontal displacement of range block (model polygon) | Horizontal component of fault slip (data) | Timing of slip | Rate of deformation (horizontal component of fault slip/ duration) | Direction of motion | Data Used | Source | Cumulative path displacement (+- cumulative error) |
| San Pitch/Gunnison (1) | 4 km | 4 km +-2 | ~18-0 Ma | 0.22 km/my | E-W | stratigraphic separation | Hintze, 1973 | 4 km +-2 |
| Canyon/Levan and Fayette segments, Wasatch fault (2) | 5 km | 5 km +- 2 km | ~10 -0 Ma | 0.5 km/my | E-W | Holocene vertical offset rates and Miocene exhumation rates, assume ~30° dip | Neimi et al., 2004; Machette et al., 1992; Jackson, 1991; Smith and Bruhn, 1984; | 6 km +-3 km |
| Cricket Range/Sevier Desert Detachment (3) | 34 km | 40 km +- 2 km | ~18-0 | 2.22 km/my (total) | E-W | Matching CR culmination in surface and subsurface. | Coogan and DeCelles, 1996; Coogan et al., 1995 | 46 km +- 3.5 km |
| | 12 km | 12 -10 km | ~19-15 Ma | 3 km/my | | AFT cooling ages assuming a 35-40 degree fault: | Stockli et al. 2001 | |
| | 22 km | 16-30 km | 15-0 Ma | 1 km/my | | | Stockli et al. 2001 | |
| House Range/"Reflection F" fault (4) | 3.33 km | 4 km +- 1km | ~15 Ma | .267 km/my | E-W | offset reflector on seismic line | Allmendinger et al., 1986 | 50 km +- 3.6 km |
| Confusion Range/House Range fault (5) | 4.66 km | 4 km (2-3 km exhumation) | ~15 Ma | | E-W | AFT cooling age | Stockli, 1999 | |
| Snake Range/northern Snake Range decollement (6) | 30 km (25-35)<br>22 km (0-18) | 30 km +-3 km (0)<br>22 +- 3 km | 35-25 Ma<br>(pause 25-18 Ma)<br>18-0 Ma | 3 km/my from 35-25<br>2 km/my from 18-0<br>3 km/my from 18-14<br>1.7 km/my from 14-0 | E-W | map relations stratigraphic offset, Ar/Ar cooling ages and AFT data (suggests 10.5-13 km of slip between 18-14 Ma ) | Gans and Miller,1983; Bartley and Wernicke 1984; Lee 1995; Miller et al., 1999; Lewis et al. 1999 | 102 km +-5.5 km |
| Schell Creek Range/Spring Valley fault (7) | 11 km (0-18) | 11 km +- 2 km | 18-0 | 1.6 km/my from 35-25<br>.6 km/my from 18-0 | E-W | map relations, AFT, ZFT, Ar/ Ar | Bartley and Wernicke 1984; Gans et al., 1985; Lee 1995; Miller et al., 1999; Lewis et al. 1999 | 113 km +- 6 km |
| Butte Mtns/Egan Range low-angle faults (8) | 16 km (25-35) | 16 km +- 2km<br>5 km exhumation | 35-25 Ma<br>16-17 Ma | | E-W | | Bartley and Wernicke 1984; Gans et al., 1985; Lee 1995; Stockli, 1999 | 129 km +- 6 km |
| Egan Range to Shoshone Mountains (9-14) | 45.6 km | 47 km +- 10 km (26 excluding Toiyabe range) | 16-0 Ma | 26 km/16 my/5 ranges | E-W | map relations and cross section restoration. | Smith et al., 1991 | 176 km +-11.8 km |
| Pine Range/Grant Range and Buck Range faults(9) | 5 km | 6 km +- 1.5 km<br>~5 km exhum. | ~15 Ma | .325 km/my | E-W | " | Lund et al.,1993; Taylor et al., 1989 | |
| Diamond Range/Pancake Range/Mahogany Hills faults (10) | 5 km | 5 km of 26 total | unknown, assumed ~16-0 | .325 km/my | E-W | map relations and cross section restoration. | Smith et al., 1991 | |
| Sulfur Springs Range faults (11) | 5 km | 5 km of 26 total | assumed ~16-0 | .325 km/my | E-W | " | Smith et al., 1991 | |
| Toquima Range/Simpson Park Mountains fault (12) | 5 km | 5 km of 26 total | assumed ~16-0 | .325 km/my | E-W | " | Smith et al., 1991 | |
| Toiyabe Range faults (13) | 5 km (25-35)<br>16 km (0-16) | 21 km extension ~5 km exhum. | 35-25 Ma<br>16-0 Ma | .5 km /my (35-25)<br>1km/my (16-0) | E-W | " | Smith , 1992; Stockli, 1999 | 176 km +-11.8 km |
| Shoshone Mountain faults (14) | 4.6 km | 5 km of 26 total | assumed ~16-0 | .325 km/my | N 64 W | " | Smith et al., 1991 | |
| Paradise Range fault(15) | 3.5 km | 3 km +-1 | assumed ~16-0 | .188 km/my | N 65 W | Paradise, C. Alpine and Sweet Water Ranges represent 100 km area that has | geographical extent on map | 179 km +- 11.8 |
| C. Alpine Range fault (16) | 3 km | 3 km +-1 | assumed ~16-0 | .188 km/my | N 65 W | extended an unknown amount | | 182 km +- 11.8 |
| Sweet Water Range fault (17) | 1.5 km | 3 km +-1 | assumed ~16-0 | .188 km/my | N 65 W | unknown/ best estimate | | 185 km +- 11.8 |
| Gillis/ Gabbs Valley Range. Gumdrop hills, Indian head, Benton spring, Petrified Spring faults.(18) | 42 km (N 12 W) | 54 +-6 km right lateral | younger than 25 Ma | 6.75 km/my (if since 8 Ma) | N 14 W | offset of steep beds (Triassic age), granite intrusions and tuffs | Hardyman et al., 1984 | 203 km +- 13.3 |
| Northern Walker Lane fault system(18) | 29 (0-6)<br>13 (8-10) | 35 +- 5 km right lateral | younger than 25 Ma | 5-10 km/my (if since 5Ma) | N 37 W | offset segments of E trending Oligocene paleovalley | Faulds et al., 2003 | |
| Wassak Range fault system(19) | 16 km | 11.76 +-1 km (13.3+-3) km | 15-present | | E-W | cross section restoration plus unroofing of granite | Surpless,1999; Stockli et al., 2002 | 215 km +-13.6 |
| | 10.5 km | 8.71 km | 14-15 | 4.3 km/my | E-W | from valley between Singatse | " | |
| | 2 km | 2.1 km | 9-7 Ma | 1.05 km/my | E-W | and Wassak | " | |

| | | | | | | | | |
|---|---|---|---|---|---|---|---|---|
| | 3.4 km | 0.5 km (0+- 2)<br>2.5 +-2 | 7-0 Ma | .3 km/my | E-W | | " | |
| Singatse Range fault system (20) | 15.66 km | 13 +-2 | 15 to present | | | offset volcanic and sedimentary rocks, Ar/ Ar isotope ages | Dilles and Gans (1995) | 228 km +-13.8 |
| | 7.66 km | main phase 7.26 | 14-12 | 3.63 km/my | E-W | | " | |
| | 4.4 km | 1.7 km | 11-8 Ma | .56 km/my | E-W | | " | |
| | 3.6 km | 4.1 km | 7-0 Ma | .58 km/my | E-W | | " | |
| Buckskin Mts/ Pine Nut Valley/ Pine Nut Range faults (21) | 5 km | 7 +- 2<br>2-3 km of exhumation | 10-0 ?? | .7 km/my | E-W | offset from mapped units; timing (10-5) from Surpless | Hudson and Oriel, 1979; Stockli, 1999 | 231 km +- 14 |
| total extension | 236 km | 235 +- 14 km | | | N 78° W | | | |

| | | | | | | | | |
|---|---|---|---|---|---|---|---|---|
| Central Basin and Range latitude of 38° N | | | | | | | | |
| Range/fault | Horizontal displacement of range block (model polygon) | Horizontal component of fault slip (data) | Timing of slip | Rate of deformation (horizontal component of fault slip/ duration) | Direction of motion | data used | References | cumulative displacement of fault slip data. (+- cumulative error) |
| Mormon Mountains area/ Mormon Peak, Tule Springs and Castle Cliff detachments (22) | 68 km | 54 +- 10 | 16-12 | 13.5 km/my | S 60 E | cross section reconstruction through Beaver Dam/ Tule Springs and Mormon Peak detachment systems | Axen et al., 1990 | 54 km +- 10 |
| Gold Butte/ South Virgin Mountains detachment (23) | 18 km | 15+-5 | ~17-15 Ma | 7.5 km/my | E-W | cross section reconstruction, AFT cooling ages, overlapping 15 Ma basalt | Wernicke et al., 1988; Brady et al., 2000; Fitzgerald et al., 1991 | 15 km +- 5 |
| Frenchman Mountain/ Lake Mead fault system (24) | 60 km | 60 min 90 max<br>65 +- 15 | 16-12 | 16.25 km/my | N 75 E | megabreccia from Gold Butte, pinchout of Mz formations, Virgin Mountains detachment system | Snow and Wernicke, 2000; Duebendorfer et al., 1992;1998; Wernicke et al., 1988 | 80 km +- 16 |
| Spring Mountains/ Las Vegas fault system (25) | 8 km | 8 km +-8 | 15-11 | | N 75 E | unknown amount of extension between Spring Mountain and Frenchman Mtn. | Wernicke et al., 1988 | 88 km +- 18 |
| Las Vegas shear zone | undetermined | 47+- 7 km | 15 -11 Ma | 11.75 km/my | | alignment of Gass Peak thrust (Sheep Range) with Wheeler Pass thrust (Spring Mt.). | Snow and Wernicke, 2000, Burchfiel et al.,1987, Wernicke et al. 1988 | |
| Sheep Range, Pintwater Range, Spotted Range detachment (26) | 23 km | 20 +-5 km | 13 Ma-? (9) | 3.67 km/my | N 63 W | extension associated with the Sheep Range detachment, extension amount based on cross section restoration | Guth, 1989; Snow and Wernicke, 2000; Snow, 1992 | 74 km +-11 |
| Nopah Range, Resting Spring Range, Spring Mtns. detachment (27) | 26 km | ~25 +- 3 km | 14-9 Ma | 5 km/ my | N 63 W | alignment of the trace of the Wheeler Pass thrusts with respect to other thrusts in in the system | Wernicke et al., 1988, Snow and Wernicke, 2000 | 113 km +-18 |
| Cottonwood, Panamint, Black Mountains/ Amargosa, central Death Valley, Emigrant detachments (28,30,32) | 102 km | 104 km | 11-2 (?) Ma | 11.5 km/ my | N 67 W | the original extent of Eagle Mountain Formation must have been within 20 km of source area in southern Cottonwoods. | Neimi et al., 2001 | 217 km +- 19 |
| Resting Springs, Nopah Ranges and Black, Panamint Mountains/ Grapevine, Amargosa, central Death Valley area detachments (27, 28, 30) | 105 km | 100 +- 7 | 9-5 Ma | 22.5 km/my | N 78 W | Willow Spring pluton intruded (10-12 km) at 11.6 cooled rapidly (6-7 Ma) and appears in boulders at ~5 Ma. (Amargosa chaos). Alignment of thrust-belt structures | Wernicke et al., 1988; Snow and Wernicke, 2000; Holm et al., 1992; Holm and Dokka, 1993; Snow, 1992. | |
| Kingston Range/Kingston Range detachment (29) | 6 km | 6 km | 13.1 Ma- 12 Ma | 6 km/my | E-W | deposition in the Shadow Valley Basin | Fowler and Calzia, 1999 | |
| Southern Black Mountains/ Kingston Range, Amargosa detachments (30) | 25 km | 25 +-3 km | 12 - 8 Ma | 6.25 km/my | E-W | granite megabreccias (in the greater Amargosa basin) possibly derived from a displaced portion of Kingston Range pluton (west of basin). | Snow and Wernicke, 2000 | |
| Funeral, Grapevine Mountains/ Point of Rocks detachment (31) | undetermined | ~10 km | 14- 10 Ma | 2.5 km/my | N 45 E | opening of the extensional Bullfrog Basin | Cemen et al., 1985; Snow and Lux, 1999 | |
| Grapevine Mountains, Bare Mountain/ Bullfrog detachment(31) | 60 km | 52 +-2 | 14-7 | 7.43 km/my | S 68 E | Cordillera fold-thrust belt reconstructions | Snow and Wernicke, 2000; 1989 | |
| Grapevine Mountains, Funeral Mountains/ Boundary Canyon detachment (31) | 32 km | 35 +- 2 km | 9-5 Ma | 8.75 km/my | S 37 E | Cordillera fold-thrust belt reconstructions, AFT, ZFT and sphene FT cooling ages | Snow and Wernicke 2000; 1989, Snow 1992, Hoisch and Simpson, 1993, Holm and Dokka, 1991 | |
| Northern Death Valley | | 20 +-10 | 5- present | 2-6 km/my | E-W | offset thrust fault and Quaternary markers | Reheis 1993, Reheis and Sayer, 1997 | |
| Cottonwood Mountains/ Emigrant fault system (32) | 22 km | 22 +- 3 km | 6-3.2 Ma | 5.5 km/my | S 45 E | correlation of White Top backfold in Cottonwood, Funeral Mountains and Specter Range. | Wernicke et al., 1988; Snow, 1992; Snow and Lux, 1999; Snow and Wernicke, 2000 | |
| Darwin Plateau, Inyo Mountains /Hunter fault (33) | 9 km | 9 +- 1 | 4.8 - 0.6 | 2.25 km/my | S 55 E | correlation of Saline Range volcanics | Burchfiel et al., 1987 | 226 km +- 19 |

| | | | | | | | | |
|---|---|---|---|---|---|---|---|---|
| Sierra Nevada/ Owens Valley fault system (34) | ~9 km | 9 +- 6 | 0-4 | 2.25 km/my | S 60 E | estimate of 15% +- 10% extension | Wernicke et al., 1988 | 235 km +- 20 |
| | 232 km | | 235 +- 20 km | | N 78° W | | | |

| Southern Basin and Range | | | | | | | |
|---|---|---|---|---|---|---|---|
| Range/fault | Horizontal displacement of range block (model polygon) | Horizontal component of fault slip (data) | Timing of slip | Rate of deformation (horizontal component of fault slip/ duration) | Direction of motion | data used | References |
| McCullough Range to Colorado Plateau (35) | 80 km | 50-80 km | 14-16 Ma (24) | 8 km/my | S 75 W | restoration of strike slip fault offsets, tilted volcanic rocks, porphyry copper emplacement depths | Spencer and Reynolds, 1989; John and Foster, 1993. |
| Black, Eldorado Mountains (36) | 36 km (total) | >25 km | 15-13.4 vlocanics | 2.5 km/my | N 70 E | tilted volcanic rocks. | Foster et al., 1993; Spencer et al., 1995; Spencer and Reynolds, 1989. |
| Sacramento, Chemehuevi Mountains (37) | 36 km | >25-30 km | 21- 15 Ma | 5 km/my | S 60 W | Ar/Ar, AFT cooling ages | John and Foster, 1993. |
| Buckskin, Rawhide Mountains (38) | 66 km | 66 +- 8 | 27-13 Ma | 4.7 km/my | S 57 W | timing indicated by tilted volcanic strata, magnitude determined by offset necessary to expose lower plate | Scott et al., 1998; Foster et al., 1993; Spencer et al., 1995; Spencer and Reynolds, 1991. |
| Catalina, Rincon Mountains (39) | 28 km | 20-30 km could be up to 40 km | 27-20 | 4 km/my | S 60 W | correlation of Precambrian granite and pre-mid-Tertiary thrusting | Davy et al. 1989; Dickinson, 1991; Fayon et al. 2000. |
| Harquahala, Harcuvar Mountains (40) | 66 km | 67 +- 17 | 26-14 Ma | 5.6 km/my | S 57 W | displaced breccias. (55 km) plus additional extension in volcanic and Precambrian rocks (12 +-7) | Richard et al., 1990; Spencer and Reynolds, 1991. |
| Pinaleno Mountains (42) | 22 km | 20-30? | 29-19 Ma | 2.5 km/my | S 60 W | Ar/Ar cooling ages, approximate amount of displacement necessary to expose lower plate | Long et al., 1995 |
| South Mountain (43) | 50 km | | 25-19 | | S 60 W | | Reynolds, 1985 |
| Whipple Mountain (44) | 63 km | 71 +- 19 | 22-16 | 11.8 km/my | S 57 W | offset of dike swarm, tilted sedimentary strata, | Davis and Lister, 1988; Spencer and Reynolds, 1991. |
| Rio Grand extension (45) | 7 km | 6 km | 12-18 Ma | .875km/my | 38° N | | Chapin and Cather, 1994; Ingersoll, 2001; Russell and Snelson, 1994 |
| | 13 km | 10 km | 12-18 Ma | 1.625 km/my | 36° N | | Chapin and Cather, 1994; Ingersoll, 2001; Russell and Snelson, 1994 |
| | 17 km | 17 km | 12-18 Ma | 2 km/my | 35° N | | Chapin and Cather, 1994; Ingersoll, 2001; Russell and Snelson, 1994 |

| Mojave | | | | | | | | |
|---|---|---|---|---|---|---|---|---|
| Fault | Horizontal displacement of range block (model polygon) | Horizontal component of fault slip (data) | Timing of slip | | | data used (offset features) | References | cumulative displacement of right lateral fault slip data. (+- cumulative error) |
| Central Mojave (41) | 63 km | 40-50 km | 24-18 Ma | 7.5 km/my | | offset features that include Jurassic dikes, intrusive rocks and shelf to ocean facies transition | Glazner et al., 1989; Martin et al., 1993; Fletcher et al., 1995; Ingersoll, 1996. | |
| Aztec Mines Wash fault | 8 km | 8 km LL | post lower Miocene | | | intrusive contact between San Gabriel terrane and Cretaceous pluton | Powell, 1981 | |
| Blue Cut fault | 4 km | 6-9-9 km | | | | Antiform in gneissic foliation | Hope, 1966 | |
| Bullion/Rodman/Pisgah fault | 13 km | 6.4-14.4 km RL | | | | Kane springs fault | Dokka, 1983 | 10.4 km +- 4 km |
| Chiriasco fault | 7-16 km | 11 km LL | | | | dacite dike, and steeply dipping Red Cloud thrust fault | Powell, 1981 | |
| Chuckwalla Valley basin | 31 km (RL) | gravity low | | | | gravity data indicate complex basin structure | Rotstein et al., 1976; Richard, 1993 | |
| Cibola fault | 7 km | 7 km RL | | | | west dipping normal faults, and east dipping contact between lavas | Richard et al., 1992 | |
| Ford Lake North basin | 5 km | 3.5 km RL | | | | base of McCoy Mountains formation | Stone and Pelka, 1989 | |
| Indian Wash Basin | 7 km | 7 km RL | | | | stratigraphic separation | Richard, 1993 | |
| Iron Mountains fault | 5 km | 5.5 km RL | | | | Rock units (unspecified | Howard and Miller, 1992 | |
| Laguna fault system | 36 km | 2km RL | | | | slip estimated by estimating extension necessary for 20° dip in conglomerate | Richard, 1993 | |
| Mammoth Wash fault | ~12 km | ~9km LL | | | | intersection of greenschist with Chocolate Mountain Thrust | Dillon, 1975 | |
| Maria fault | | 4.5 km RL | | | | thrust faults and syncline | Hamilton, 1987; Ballard, 1990 | |
| Mesquite Lake fault | | 3.5 km RL | | | | folds in Pleistocene sediments | Bassett and Kupfer, 1964 | |
| Packard Well fault | 16 km | 16 km RL | | | | Mesozoic rocks and structures | Powell, 1981; Richard and Dokka, 1992 | |
| Pinto Mountain fault | not available | 18-22 km LL | | | | intrusive contacts | Hope, 1966; Dibblee, 1982 | |
| Salton Creek fault | 8 km | 8 km LL | | | | correlation with Aztec mines fault | Powell, 1981 | |
| Sheep Hole, Dry Lakes fault | 31 km | 23 km RL/11 km | to early Pleistocene | | | Photo interpretation | Powell, 1981; Howard and Miller, 1992 | |
| Valley Mountain fault | 21 km | 6.5-14.4 km RL | | | | | Dokka, 1983; Richard, 1993 | |
| Cleghorn Pass fault | valley mt offset | 12 km RL | to early Pleistocene | | | intrusive contacts | Howard and Miller, 1992 | |
| Cleghorn Lakes fault | " | 3 km RL | to early Pleistocene | | | intrusive contacts | Howard and Miller, 1992 | |
| Cadiz Lake fault | 16-25 km | 25 km RL | to early Pleistocene | | | roof pendants with distinctive lithology | Howard and Miller, 1992 | |
| Broadwell Lake fault | 6 km | 6 km RL | to early Pleistocene | | | Miocene strata | Howard and Miller, 1992 | 16 km +- 4 km |
| South Bristol fault | 9 km | 6.5 km RL | to late Pleistocene | | | Mesozoic granitites, metavolcanics | Howard and Miller, 1992 | 22.5 km +- 4 km |
| Bristol, Granite Mountain fault | 27 km | 10 km RL (0-10) | | | | unknown, or plutons and volcanic rocks | Howard and Miller, 1992; Dokka and Travis, 1990 | 27.5 km +- 6.4 km |
| Ludlow | 14 km | >6 km RL | to early Pleistocene | | | conglomerate | Howard and Miller, 1992 | 33.5 km +- 6.4 km |
| Calico | 10 km | 9.6 km RL | | | | offset early Miocene fault | Dokka, 1989; Glazner et al., 2002 | 43.1 km +- 6.4 km |
| Blackwater | 4.5 km | 1.8 km | last 3.77 m.y. | | | offset volcanics, basement lithologies | Oskin et al., 2004 | |
| Gravel Hills + Harper Lake | 12.5 km | 3.2 km RL + 3km RL | | | | offset lithologies | Dokka and Travis, 1990; Dibblee, 1968 | |
| Camp rock | 11 km | 4 km RL | | | | offset basement lithologies | Dokka, 1983; Dibblee, 1964 | 47.1 km +- 6.4 km |
| Hendale | 4 km | 3 km RL | | | | offset lithologies | Miller and Morton, 1980 | 50.1 km +- 6.4 km |
| Lockheart | 4 km | >0 RL | | | | | Dokka and Travis, 1990 | |
| Lenwood | 5 km | 2 km RL | | | | offset volcanics, graben width | M. Strane, Pers. Comm,2005 | 53 km +- 6.4 km |
| NE Mojave rotation | 23 km | 22-33 km RL | | | | paleomagnetic rotations | Schermer, 1996; Miller and Yount, 2002 | |
| total shear in the Mojave | 99 km | 53 +- 6.4 km | | | | | | |

| Rotations | | amount | age | rate | direction | | References |
|---|---|---|---|---|---|---|---|
| Colorado Plateau (45) | 1.5° | 1°-1.5° | 12-18 Ma | .1875°/my | cw | paleomagnitism, extension determined through cross section restoration | Chapin and Cather, 1994 |
| Eastern Transverse Ranges (46) | | 41.4 ° +-7.7 | after 10.4 Ma | | cw | paleomagnetic data | Carter et al., 1987 |
| Northeastern Mojave (47) | | 23° locally 63° | after 10.4 Ma | | cw | paleomagnetic data | Schermer et al., 1996 |
| Jurassic dikes in NE Mojave (47) | | 40-50 ° | | | cw | | Ron and Nur, 1996 |
| Mojave rotations (47) | | 30° | 24-18 Ma | | cw | paleomagnetic data | Dokka and Travis, 1990; Dokka et al., 1998 |
| Cottonwood and Funeral Mts (31,32) | | 40° | mid Miocene or later | | cw | paleomagnetic data | Snow and Lux, 1999; Snow and Wernicke, 2000 |
| Black Mountains (30) | | 50-80° | after mid Miocene pluton | | | paleomagnetic data | Holm et al., 1993 |
| Grapevine Mountains (31) | | ~20° | | | ccw | paleomagnetic data | Niemi, 2002; Snow and Wernicke, 2000 |
| Bare Mountain (31) | | 80° | pre mid-Miocene | | cw | paleomagnetic data | Snow and Prave, 1994 |
| Pintwatrer, Spotted and Specter Range and Stripped Hills (26) | | oroclinal flexure (75-90°) | between 16 and 14 | | cw | | Carr et al., 1986; Hudson et al., 1994; Niemi, 2002. |
| Sierra Nevada (34) | | 6° +-8° | post Cretaceous | | cw | paleomagnetic data | Frei et al., 1984; Frei, 1986; Bogen and Schweickert, 1985 |
| western Transverse Ranges | 117° | 90°-110° | ~15 Ma | 6° /my | cw | paleomagnetic data | Hornafius et al., 1986; |

| Western San Andreas tie points | | | | | | | |
|---|---|---|---|---|---|---|---|
| | | | | | | | |
| Range/fault | Horizontal displacement of range block (model polygon) | Horizontal component of fault slip (data) | Timing of slip | Rate of deformation (horizontal component of fault slip/ duration) | Direction of motion | data used | References |
| San Andreas motion (48) | 310 km<br>0-6 Ma 174 km<br>8-12Ma 89 km<br>14-16Ma 47 km | 315 km +- 10 | 0-5 Ma 170 km +-5<br>0-10 Ma 289 km +-9<br>0-16 Ma 315 km +-10 | 0-5 Ma 34 km/yr 0-10 Ma 24 km/yr 0-16 Ma 4.3 km/yr | N 30 W | offset of Holocene geological features, Early Miocene volcanic and sedimentary rocks and Miocene sedimentary breccias. | Atwater and Stock, 1998; Dickinson and Wernicke, 1997; Dickenson, 1996; Graham et al., 1989; Sieh and Jahns, 1984; Matthews, 1979 |
| Baja/ Isla de Tibron (49) | 260 km | 255 km +- 10 | 6-0 Ma | 43.5 km/yr | N 50 W | correlating Miocene volcaniclastic strata | Oskin et al., 2001 |
| western Transverse Ranges | | | | | | | |
| _Eocene Poway Group | | places San Miguel, Santa Rosa and Santa Cruz Islands just north of San | | | | correlation of distinctive volcanic clasts with source area in Sonora Mexico | Abbott and Smith, 1989 |
| _Borderland extension | 305 km at N 67 W | ~250 km | ~18 Ma | 14 km/my | ~N 40 W | seismic reflection data, correlation of "mega key-beds" | Crouch and Suppe, 1993; Bohannon and Geist,1998 |